1

Metallabenzenes and Fused-Ring Metallabenzenes of Osmium, Ruthenium and Iridium: Syntheses, Properties and Reactions

*Benjamin J. Frogley, Warren R. Roper and L. James Wright**

School of Chemical Sciences, University of Auckland, Auckland, New Zealand

1.1 Introduction

The origin of metallabenzenes can be traced back almost two centuries to the discovery of benzene by Michael Faraday in 1825 [1]. He managed to separate benzene from the oily liquid obtained as a by-product during the manufacture of an "illuminating gas" by the destructive distillation of fish or whale oil. He correctly described a wide range of its properties and identified the formula as two proportions of carbon to one proportion of dihydrogen gas – thus describing it by the name "bicarburet of hydrogen". A few years later, in 1833, it was also isolated by the German chemist Eilhard Mitscherlich by the distillation of benzoic acid from gum benzoin. Mitscherlich correctly noted that it was identical to Faraday's bicarburet of hydrogen and gave it the name "benzin", from which the common name benzene is derived [2].

The molecular structure eluded chemists for many years. It was not until 1865 that German scientist Friedrich August Kekulé proposed the six-membered cyclohexatriene ring structure with alternating single and double bonds which subsequently led to the development of the concept of aromaticity [3, 4]. These advances revolutionised organic chemistry and began a flood of research into this exciting new area of so-called aromatic chemistry. Benzene is now considered the archetypical aromatic compound, and it is often used as the yardstick against which other species are compared with regard to aromatic character. While a precise definition of "aromaticity" remains somewhat nebulous, properties associated with benzene that have been classically used to characterise aromaticity include planarity, bond length equalisation, π-electron delocalisation, aromatic stabilisation energy, diamagnetic ring currents and electrophilic substitution, rather than addition, reactions. In more recent times, determinations of aromatic stabilisation energies by computational methods have been used to obtain more tangible measures of aromaticity.

Heteroaromatic species could be considered the next generation of aromatic compounds to be discovered. Amongst this large class of compounds, there are many

*Corresponding author: lj.wright@auckland.ac.nz

Metallabenzenes: An Expert View, First Edition. Edited by L. James Wright.

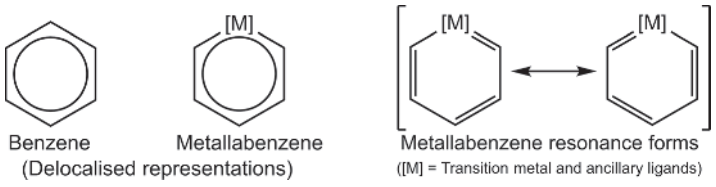

Chart 1.1 Metallabenzene delocalised representation and contributing resonance forms.

six-membered heterocycles that can be thought of as benzene analogues in which one CH unit of benzene has been formally replaced by an appropriate heteroatom. Pyridine, with the heteroatom nitrogen, was one of the earliest examples, and Scottish scientist Thomas Anderson is credited with the first report of this compound in 1849 [5]. Since then, related benzene analogues incorporating a wide array of main group heteroatoms have been isolated and these include, but are not limited to, phosphorus [6, 7], arsenic [7, 8], silicon [9], antimony [10], bismuth [10], germanium [11] and tin [12].

Metallabenzenes, which are perhaps the third generation of related aromatic compounds, have arrived comparatively recently in this timeline. The notion of formally replacing one CH unit of benzene with an appropriate transition metal (and its ancillary ligands) was proposed theoretically in 1979 by Thorn and Hoffmann [13] and it was only a short three years later before the first metallabenzene, an osmabenzene, was synthesised and characterised by Warren Roper and co-workers in New Zealand [14]. The aromatic character of this and other metallabenzenes (Chart 1.1) has now been thoroughly established through a range of different computational methods, and these are discussed in detail in Chapter 7 of this book. From these beginnings a new class of aromatic compounds, the metallabenzenes, was born.

In this chapter we provide a personal perspective on the contributions our group has made to this field, including studies of the syntheses, properties and reaction chemistry of osma-, ruthena- and iridabenzenes as well as related fused-ring derivatives.

1.2 Syntheses and Properties of Metallabenzenes with Methylthiolate Substituents

1.2.1 Osmabenzenes

In the 1970s and early 1980s, there was an acceleration of research efforts focused on the organometallic chemistry of transition metals, particularly on species where a transition metal is multiply bonded to a carbon donor ligand. We had been working in this area for some time and had developed a number of new carbene [15, 16], carbyne [17, 18] and thiocarbonyl [19–21] complexes of second- and third-row transition metals. We were aware of the 1979 theoretical paper by Thorn and Hoffmann that briefly describes the possibility of metallabenzenes as stable species [13]. Therefore, a few years later, when we were exploring the coordination of ethyne at the osmium centre of the zero-valent complex $Os(CS)(CO)(PPh_3)_3$, it did not take long for us to realise the CS ligand and two ethyne molecules had cyclised at the metal centre to produce the first metallabenzene, the osmabenzene, $Os(C_5H_4\{S\text{-}1\})(CO)(PPh_3)_2$ (**1**) (Scheme 1.1). In this

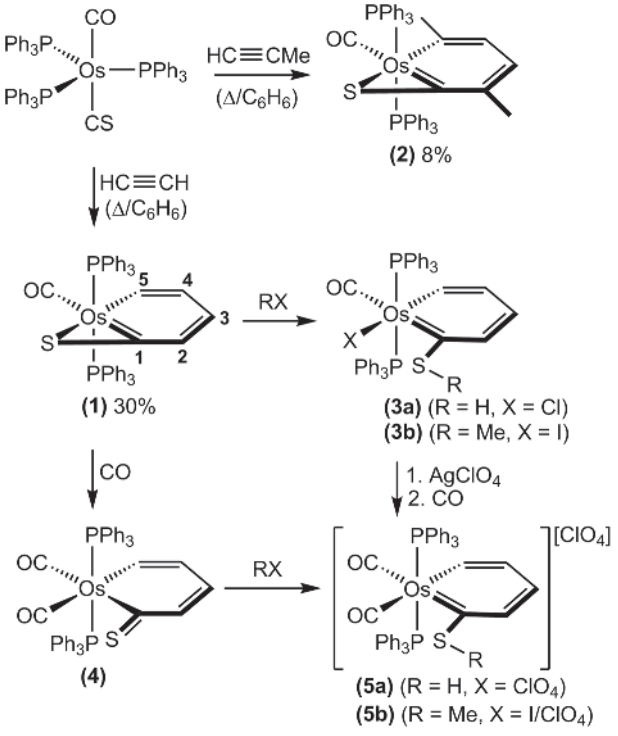

Scheme 1.1 Preparation of osmium complexes **1–5**.

compound the six-membered metallacyclic ring comprises the thiocarbonyl carbon atom, the four carbons of the two ethyne molecules and the osmium atom. The sulfur atom is also coordinated to the osmium metal centre, generating a secondary three-membered Os–C–S osmathiirene ring [14]. Therefore, the osmabenzene **1** could also formally be considered an osmabenzothiirene [22].

To synthesise the osmabenzene **1**, a solution of $Os(CS)(CO)(PPh_3)$ in benzene or toluene was treated with a slow stream of ethyne at 70°C for 20 min. Dark-brown crystals of pure **1** were formed in around 30% yield following purification by recrystallisation from *n*-hexane and column chromatography of the solid obtained [23].

This reaction can be considered a formal [1+2+2] cyclisation at the osmium centre of two molecules of ethyne and the carbon of the CS ligand. The most likely mechanism has been determined computationally using the model complex $Os(CS)(CO)(PH_3)_3$ [24]. The adduct **1A** (Scheme 1.2) is formed by coordination of the first molecule of ethyne after phosphine dissociation. The thiocarbonyl and ethyne ligands then combine to give the osmacyclobutenethione **1B**. The propensity of ligands such as CS to engage in cyclisation and migratory insertion reactions has proven to be invaluable in the synthesis of a number of metallaaromatic compounds. Coordination of the second molecule of ethyne, to give **1C**, and subsequent insertion of both carbon atoms into the four-membered ring gives the osmacyclohexadienethione **1D**. Finally, coordination of the sulfur atom to osmium results in aromatisation of the six-membered ring and formation of the osmabenzene **1**.

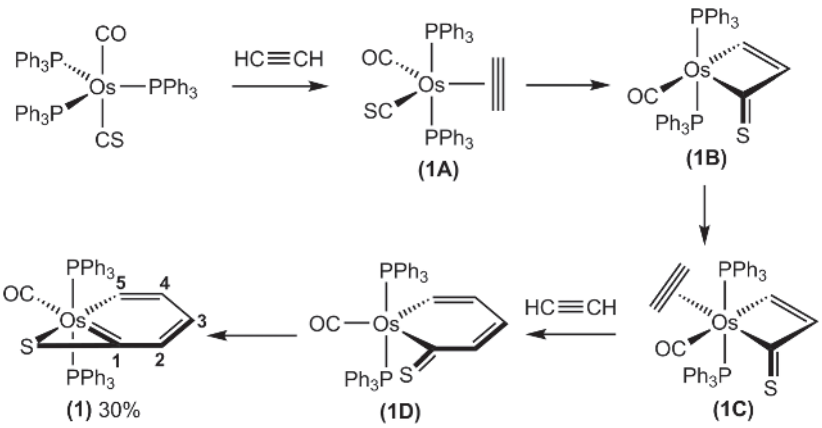

Scheme 1.2 Proposed mechanism for the synthesis of the osmabenzene **1** based on computational studies using PH_3 model compounds.

This cyclisation reaction is not limited to ethyne, and later we found the related dimethyl-substituted osmabenzene $Os(C_5H_2\{S\text{-}1\}\{Me\text{-}2\}\{Me\text{-}4\})(CO)(PPh_3)_2$ (**2**) (Scheme 1.1) is formed as dark-brown crystals when $Os(CS)(CO)(PPh_3)_3$ is treated with propyne, albeit in the low yield of 8%. The major product from this reaction is the complex $OsH(C{\equiv}CMe)(CS)(CO)(PPh_3)_2$ which arises from the simple C–H oxidative addition of propyne. Fortunately, this can be easily separated from the metallabenzene **2** by column chromatography and isolated in 23% yield [25].

Our original report of the first metallabenzenes also included several derivatives of **1** which could be prepared through reactions in which the osmium–sulfur bond was cleaved. The sulfur atom in **1** is nucleophilic and readily undergoes protonation with hydrochloric acid or alkylation with methyl iodide to give the neutral osmabenzenethiol **3a** or the methylthiolate-substituted osmabenzene **3b**, respectively (Scheme 1.1). The sulfur atom in **1** is also displaced from osmium on treatment with carbon monoxide. The resulting osmacyclohexadienethione, **4**, does not have the same π-bond delocalisation about the six-membered ring that is present in **1**, but this can be returned by protonation or alkylation of the thione sulfur. Thus, treatment of **4** with perchloric acid or methyl iodide followed by crystallisation in the presence of sodium perchlorate gives the corresponding osmabenzenes **5a** or **5b**, respectively, which are the cationic analogues of **3a** and **3b** (Scheme 1.1) [14]. **5a** or **5b** can be prepared by an alternative route starting from **3a** or **3b**, respectively, as indicated in Scheme 1.1.

A key question that had to be addressed in the original paper describing the osmabenzene **1** was whether it was best described as a metallabenzene with delocalised π-bonding or, alternatively, as an osmacyclohexatriene with localised double bonds. Key information that strongly supported a delocalised π-system was provided by the single crystal X-ray structure determination (see Figure 1.1). The structure of **1**, and later **2** (Figure 1.2), showed a planar six-membered metallacyclic ring with similar carbon–carbon bond lengths that were midway between standard sp^2 carbon–carbon single (1.46 Å) and double (1.34 Å) bonds. Importantly, the two osmium–carbon bonds were essentially equal in length and midway between those of typical single and double osmium–carbon bonds [26]. Since ring planarity and bond length equalisation are both

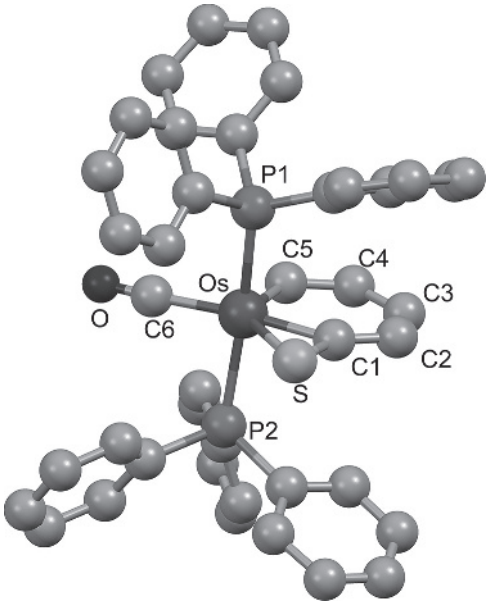

Figure 1.1 Molecular structure of osmabenzene **1**. Hydrogen atoms have been omitted for clarity. Selected distances [Å]: Os–C1 2.00(1), Os–C5 2.00(1), Os–S 2.474(3), Os–C6 1.92(1), C1–C2 1.36(2), C2–C3 1.38(2), C3–C4 1.42(2), C4–C5 1.39(2).)

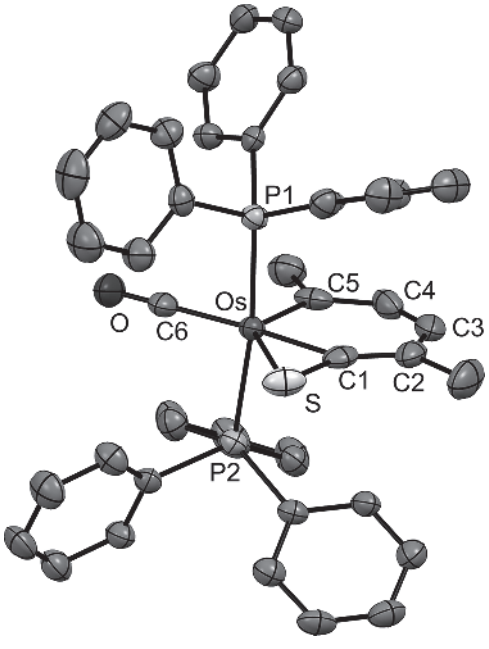

Figure 1.2 Molecular structure of osmabenzene **2** showing 50% probability thermal ellipsoids. Hydrogen atoms have been omitted for clarity. Selected distances [Å]: Os–C1 2.027(4), Os–C5 2.022(5), Os–S 2.4990(12), Os–C6 1.908(4), C1–C2 1.365(6), C2–C3 1.400(7), C3–C4 1.385(7), C4–C5 1.415(6). (*See color plate section for the color representation of this figure.*)

classic indicators of aromatic character, the structural data (together with the low field chemical shifts of the ring protons and carbon atoms in the ^{1}H and ^{13}C NMR spectra) [23] strongly supported a metallabenzene formulation for **1**.

Regarding the η^2-C(S) moiety in both **1** and **2**, the Os–S bond lengths (2.474(3) and 2.4990(12) Å, respectively) are slightly longer than normal Os–S single bonds, while the C–S bond lengths, (1.66(1) and 1.689(6) Å, respectively) are slightly shorter than standard C–S single bonds. These observations suggest that in both complexes the sulfur atom is not strongly bound to the metal centre [14, 25].

An X-ray crystal structure determination has also been obtained for the osmabenzene $Os(C_5H_4\{SMe\text{-}1\})Cl(CO)(PPh_3)_2$, an analogue of **3b** which has a chloride rather than iodide ligand. The structural parameters associated with the osmabenzene ring in this complex display the same key features found for **1** and **2**, i.e. near bond length equalisation and ring planarity (Os–C1 2.109(3), Os–C5 2.027(3), C1–C2 1.412(4), C2–C3 1.371(4), C3–C4 1.393(5), C4–C5 1.368(4) Å) [27].

The NMR spectroscopic data obtained for the osmabenzenes **1** and **2** provide important indications that a delocalised representation of the π-bonding within the metallacyclic ring is appropriate. In the ^{1}H NMR spectrum of **1**, H5, which is attached to a metal-bound carbon atom (see Scheme 1.1 for numbering system), is found at 13.95 ppm [23]. This notable down-field chemical shift is consistent with transition metal–carbon multiple bonding character and approaches, but does not quite meet the down-field shifts typically observed for related osmium carbene protons (*ca.* 18 ppm) [27]. H3 and H4 in **2** are found in the ^{1}H NMR spectrum at the "benzene-like" chemical shifts of 7.59 and 6.65 ppm, respectively.

The metal-bound carbon atoms of **2**, C1 and C5, are found at 257.43 and 220.07 ppm, respectively in the ^{13}C NMR spectrum. These considerable down-field chemical shifts are also consistent with osmium–carbon multiple bonding character. The remaining ring carbon atoms that are remote from the metal centre are observed at positions similar to those found in benzene and benzene derivatives (119.89 (C2), 147.98 (C3) and 129.22 (C4) ppm) [25]. These distinctive chemical shifts for the ring protons and carbon atoms are not limited to the osmabenzenes with the η^2-CS moiety, as is evidenced by the very similar spectra found for the methylthiolate-substituted osmabenzene $Os(C_5H_4\{SMe\text{-}1\})Cl(CO)(PPh_3)_2$ (^{1}H NMR: 6.65 (H2), 7.07 (H3), 6.57 (H4), 13.27 (H5) ppm, ^{13}C NMR: 237.4 (C1), 121.6 (C2), 145.8 (C3), 123.8 (C4), 211.0 (C5) ppm) [27].

Further general features are apparent in the NMR spectra of these and related osmabenzenes. Many of the resonances in the ^{1}H and ^{13}C NMR spectra are split into fine triplets due to coupling to the two phosphorus atoms of the mutually *trans* triphenylphosphine ligands. In most cases, coupling to the two phosphorus atoms is observed for carbons C1 and C5 in the ^{13}C NMR spectra, and $^{2}J_{CP}$ is usually in the order of 5–10 Hz. When present, the H1 and/or H5 protons will often also display coupling to phosphorus in the ^{1}H NMR spectra and this is usually in the order of 1–3 Hz. This phenomenon can sometimes also be noted in the atoms more remote from the metal, although this is much less common. In addition, the ring protons on the majority of related metallabenzenes and metallabenzenoids usually display long-range proton–proton coupling across three or more bonds in a manner similar to the *meta*-coupling often observed in aromatic organic compounds.

1.2.2 Iridabenzenes

The success encountered in synthesising these osmabenzenes was in large part due to the remarkable propensity of the thiocarbonyl ligand to undergo cyclisation and migratory insertion reactions. A natural progression was to then extend this work and prepare iridabenzenes using the same strategy. At the time this work was carried out, a number of iridabenzenes had already been reported using alternative routes, and these are discussed in Chapters 2, 3 and 4 of this book. However, it was reasoned that if the thiocarbonyl route was successfully applied to iridium it would give iridabenzenes with very different ancillary ligands and ring substituents to those that had been prepared previously.

It had already been shown that the iridacyclopentadiene complex $[Ir(C_4H_4)(NCMe)(CO)(PPh_3)_2][OTf]$ (^-OTf or triflate = $^-O_3SCF_3$) could be prepared by a cyclisation reaction involving two ethyne molecules at the iridium centre of the cation $[Ir(NCMe)(CO)(PPh_3)_2][OTf]$ [28]. This iridium cation is in turn obtained from Vaska's complex, $IrCl(CO)(PPh_3)_2$ [29], through treatment with silver triflate in acetonitrile solvent [30]. Although the CO ligand in this complex does not insert into the iridacyclopentadiene ring, we reasoned that the thiocarbonyl analogue might undergo this rearrangement to give an iridabenzene that is closely related to **1**.

We had already developed a route to the thiocarbonyl analogue of Vaska's compound, $IrCl(CS)(PPh_3)_2$ [20, 31], and so the cation, $[Ir(CS)(NCMe)(PPh_3)_2][OTf]$ (**6**), was readily accessible through treatment of this complex with AgOTf/NCMe. When a dichloromethane solution of this orange species was treated with ethyne under ambient conditions, the cationic iridacyclopentadiene complex, $[Ir(C_4H_4)(CS)(NCMe)(PPh_3)_2][OTf]$ (**7**), formed spontaneously (Scheme 1.3). This complex could be isolated as a yellow solid if the temperature was kept low (*ca*. 0°C) and precipitation carried out rapidly by addition of *n*-hexane [32]. The barrier to rearrangement of this cationic iridacyclopentadiene to the corresponding iridabenzene, through migratory insertion of the CS ligand, is relatively low. Even at 20°C, after 1 h in solution some rearrangement of **7** to the cationic iridabenzene $[Ir(C_5H_4\{S\text{-}1\})(NCMe)(PPh_3)_2][OTf]$ (**9**) can easily be detected by ^1H NMR spectroscopy. Complete conversion of **7** to the iridabenzene **9** occurs on heating **7** under reflux in dichloromethane (*ca*. 40°C) for 16 h (Scheme 1.3). In practice, if the iridabenzene is the target product, all these transformations can be carried out in one pot starting from **6** to give **9** in yields of over 90%. It is noteworthy that if chloride is added to **7** the neutral iridacyclopentadiene complex $Ir(C_4H_4)Cl(CS)(PPh_3)_2$ (**8**) is obtained, and this complex is significantly more resistant to migratory insertion of the CS ligand (Scheme 1.3). However, **8** can be converted into the iridabenzene, $Ir(C_5H_4\{SMe\text{-}1\})Cl_2(PPh_3)_2$ (**13**), by treatment with methyl triflate in a refluxing 1, 2-dichloroethane solution followed by the addition of lithium chloride (Scheme 1.3) [32–34].

The acetonitrile ligand in **9** is fairly labile and the neutral iridabenzene $Ir(C_5H_4\{S\text{-}1\})Cl(PPh_3)_2$ (**10**) can easily be prepared by the addition of chloride (Scheme 1.3) [33]. The iridabenzenes **9** and **10** can both be considered analogues of the original osmabenzene **1**.

Isolation of the intermediate **7** indicates that the reaction mechanism for the formation of iridabenzene **9** is different from that determined by computational studies for the formation of the closely related osmabenzene **1**. Formation of **9** involves cyclisation of two ethyne molecules at iridium to give the isolated intermediate iridacyclopentadiene

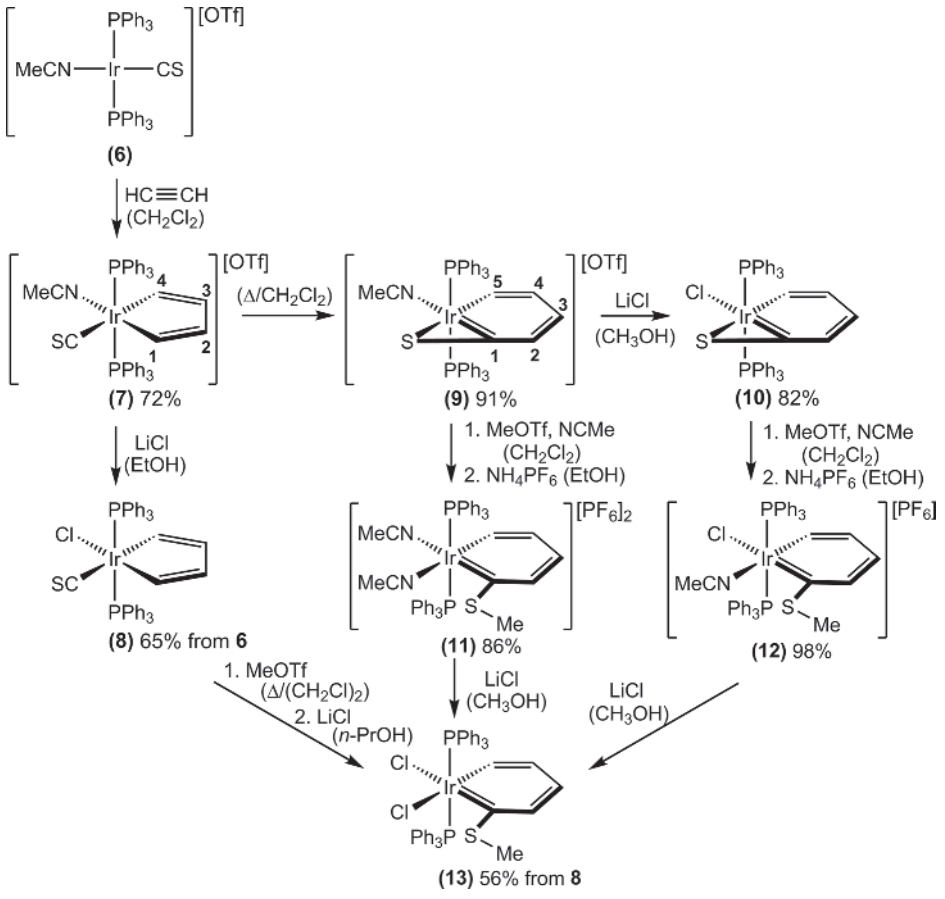

Scheme 1.3 Synthesis of the iridacyclopentadienes **7–8** and the iridabenzenes **9–13**.

7, followed by insertion of CS into an Ir–C bond to give the iridabenzene **9** [32]. In contrast, calculations predict that formation of the osmabenzene **1** occurs via cyclisation of one ethyne and CS to form an osmacyclobutenethione intermediate (**1B**; Scheme 1.2) which subsequently inserts both carbon atoms of a second ethyne to form the six-membered metallacyclic ring in **1** [24].

A number of simple derivatives of the iridabenzenes **9** and **10** are readily accessible through alkylation of the sulfur atoms with methyl triflate (MeOTf). When the methylation reaction of **9** is conducted in the presence of a small amount of acetonitrile, the maroon dicationic iridabenzene $[Ir(C_5H_4\{SMe\text{-}1\})(NCMe)_2(PPh_3)_2][PF_6]_2$ (**11**) can be isolated after addition of NH_4PF_6. Methylation of **10** under the same conditions gives the red monocationic iridabenzene $[Ir(C_5H_4\{SMe\text{-}1\})Cl(NCMe)(PPh_3)_2][PF_6]$ (**12**) (Scheme 1.3). The acetonitrile ligands in both complexes are labile, and treatment of either **11** or **12** with lithium chloride yields the neutral dichloride iridabenzene, **13**, as a purple crystalline solid (Scheme 1.3) [34].

The crystal structures of iridabenzenes **9** and **13** (Figure 1.3) have been determined and provide interesting comparisons with the structures of the osmabenzenes **1** and **2**

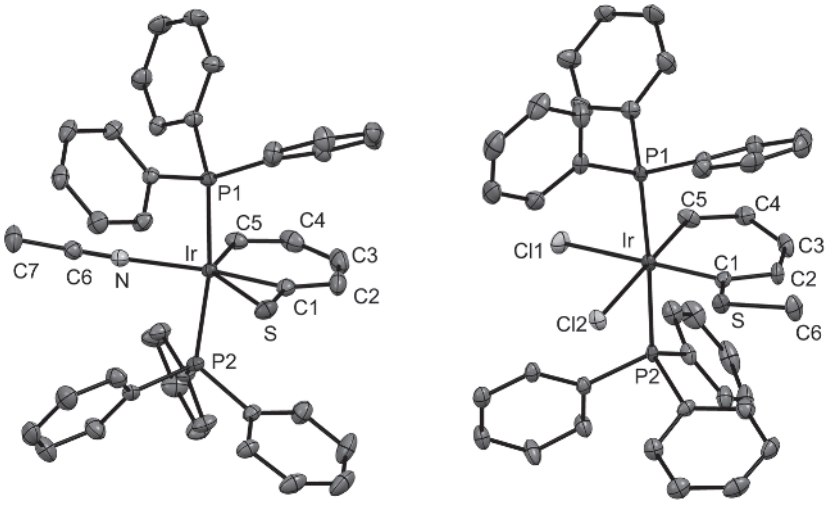

Figure 1.3 Molecular structures of iridabenzenes **9** (left) and **13** (right) showing 50% probability thermal ellipsoids. Hydrogen atoms have been omitted for clarity. Selected distances [Å] for **9**: Ir–C1 1.933(2), Ir–C5 1.989(2), Ir–S 2.6326(6), Ir–N 2.1340(16), C1–C2 1.398(3), C2–C3 1.366(4), C3–C4 1.421(4), C4–C5 1.365(3). Selected distances [Å] for **13**: Ir–C1 1.993(4), Ir–C5 1.992(4), Ir–Cl1 2.4846(10), Ir–Cl2 2.4606(11), C1–C2 1.427(6), C2–C3 1.363(6), C3–C4 1.413(6), C4–C5 1.352(6), S–C6 1.820(5).

(Scheme 1.1) and the iridacyclopentadiene **8**. The bonds within the almost perfectly planar five-membered metallacyclic ring of **8** serve as benchmarks for the lengths of (presumably) essentially localised C–C double bonds and Ir–C(sp^2) single bonds within an iridacyclic ring. The relevant distances in **8** are: iridium–carbon single bonds (Ir–C1 2.051(3), Ir–C4 2.093(3) Å), carbon–carbon double bonds (C1–C2 1.327(4), C3–C4 1.350(5) Å), and carbon–carbon single bonds (C2–C3 1.446(5) Å) [33]. The iridabenzene **9** is also very planar, with the greatest deviation from the Ir, C1–C5, S1 least-squares plane occurring for the iridium metal (0.038 Å). The iridium–carbon bonds (Ir–C1 1.933(2), Ir–C5 1.989(2) Å) are significantly shorter than they are in **8**, as would be expected if there is some multiple bond character in these bonds arising from a delocalised π-bonding system. The remaining carbon–carbon bonds in the IrC_5 ring of **9** display some alternation in their distances but all fall well between the single and double carbon–carbon bond lengths observed in **8** [32, 33]. The structural evidence for the classification of **9** as having a delocalised, aromatic π-bonding system is therefore quite compelling. The bond lengths in the neutral methylthiolate-substituted iridabenzene, **13**, follow the same trends, although in this case the iridium metal lies quite significantly (0.307 Å) out of the least squares plane formed by the iridium metal and carbons C1–C5, although the plane formed by these five carbon atoms is itself very planar[33]. While non-planarity is often associated with a loss of aromaticity in simple carbocyclic compounds, it has been shown computationally that distortions of this type do not adversely affect the aromaticity in metallabenzenes [35].

Interestingly, the sulfur atom of the η^2-C(S) moiety in **9** does not appear to interact with the iridium metal as strongly as it does with the osmium metal in the osmabenzenes **1** and **2**. The Ir–S bond length of 2.6326(6) Å is considerably longer than the Os–S

bond lengths in **1** and **2** (2.474(3) and 2.4990(12) Å, respectively), and the Ir–C1–S angle of 93.80(9)° is larger (*cf.* 84.58° and 84.00° in osmabenzenes **1** and **2**, respectively) [14, 25, 33].

In addition to the structural data, the spectroscopic data also support the notion that the iridabenzenes **9–13** are indeed aromatic. In the ^{1}H NMR spectrum of cationic **9**, H5, which is attached to the iridium-bound C5 atom, resonates at 12.47 pm. This is significantly down-field compared to the resonances of the corresponding protons (H1 and H4, which are attached to the metal-bound carbon atoms) in the iridacyclopentadiene complex **7** (7.20 and 6.53 ppm, respectively). Likewise in the ^{13}C NMR spectrum of iridabenzene **9**, the iridium-bound carbons C1 and C5 are found at the low-field positions of 243.9 and 176.9 ppm, respectively, while the iridium-bound carbons C1 and C4 in **7** are found at 152.6 and 136.0 ppm, respectively [32]. The characteristically large down-field chemical shifts that are found for the metal-bound carbon atoms in these iridabenzenes are consistent with there being multiple-bond character in each of the iridium–carbon bonds, further supporting a delocalised π-bonding system [27]. The remaining hydrogen and carbon atoms of **9** that are remote from the iridium metal centre exhibit NMR resonances in regions typical of traditional organic aromatics (^{1}H NMR: 6.24 (H2), 7.50 (H3), 6.81 (H4) ppm, ^{13}C NMR: 117.6 (C2), 153.9 (C3), 127.4 (C4) ppm) [32]. The chemical shifts found in the neutral iridabenzene **10** are very similar (^{1}H NMR: 12.45 (H1), 5.65 (H2), 6.80 (H3) and 6.54 (H4) ppm, ^{13}C NMR: 249.47 (C1), 118.71 (C2), 149.40 (C3), 125.99 (C4), 171.43 (C5) ppm).

The complexes **11–13**, which arise from methylation of the sulfur function in **9** or **10**, display very similar chemical shifts for the metallabenzene ring atoms in the NMR spectra. For example, for the dicationic **11**, H5 is found at 11.59 ppm in the ^{1}H NMR spectrum, while in the ^{13}C NMR spectrum C1 and C5 are found at 224.4 and 180.9 ppm, respectively [32]. In the neutral **13**, H5 is observed at 12.31 ppm (^{1}H NMR spectrum), and C1 and C5 at 229.12 and 198.19 ppm, respectively (^{13}C NMR spectrum). The remaining ring signals are found in the expected aromatic positions [33].

1.3 Syntheses and Properties of Fused-Ring Metallabenzenes

By the start of the 21st century the study of metallabenzenes had expanded into a diverse field featuring a variety of different metal centres and differently substituted carbon skeletons prepared via a wide range of synthetic routes. In spite of this, the sister field of fused-ring metallabenzenes, where the primary six-membered ring is fused with a secondary ring structure, was still very much in its infancy and examples with fused heterocyclic rings were very rare. We therefore directed our attention to compounds of this type.

Metallabenzofurans are now the largest class of the otherwise relatively unexplored fused-ring metallabenzenes. In all the reported examples of metallabenzofurans, the metal occupies a ring junction position and bonds to the oxygen of the fused five-membered furan ring (see Chart 1.2). In principle many other metallabenzofuran isomers are possible, but these have yet to be reported. The three important valence bond structures, as well as a delocalised representation with the general numbering scheme for the known isomer, are given in Chart 1.2.

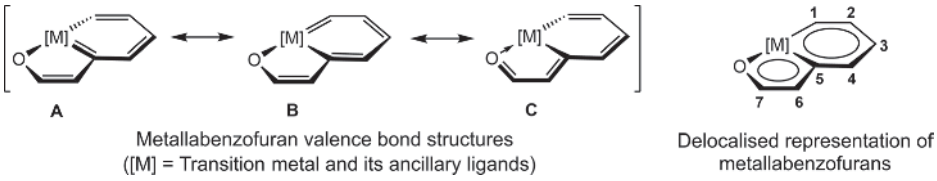

Chart 1.2 General representation and valence bond structures for the single metallabenzofuran isomer that has been reported.

1.3.1 Osmabenzofurans

The synthesis of the first osmabenzene by the reaction between two ethyne molecules and the osmium complex $Os(CS)(CO)(PPh_3)_3$ naturally led us to consider further investigations involving substituted acetylenes. The reaction with propyne to give the osmabenzene **2** has already been noted above. Interestingly, it was found that, with diphenylacetylene, only one molecule adds to $Os(CS)(CO)(PPh_3)_3$, with accompanying loss of both PPh_3 and (surprisingly) CO, to yield the osmacyclopropene complex $Os(CS)(PhC{\equiv}CPh)(PPh_3)_2$ (**14**) (Scheme 1.4) [36, 37]. This complex did not undergo further reaction with diphenylacetylene even in the presence of a large excess of this reagent. However, on treatment of **14** with CO, the coordinated diphenylacetylene could be induced to combine with the thiocarbonyl carbon to give the osmabutenethione, **15**. This very unreactive species bears some similarity to **1B** in Scheme 1.1, which has been proposed as an intermediate in the synthesis of osmabenzene **1**.

Compound **14** is remarkably stable towards further reaction with most alkynes. However, the facile reaction between **14** and CO suggested that **14** might undergo reaction with a suitably activated alkyne and this could lead to a new osmabenzene through formal [1 + 2 + 2] cyclisation of the two alkyne molecules and the thiocarbonyl ligand. One of the activated alkynes chosen for study was methyl propiolate ($HC{\equiv}CCO_2CH_3$). When **14** was heated under reflux in benzene with this alkyne, a reaction ensued but not in the way initially anticipated. The product obtained was the osmabenzofuran

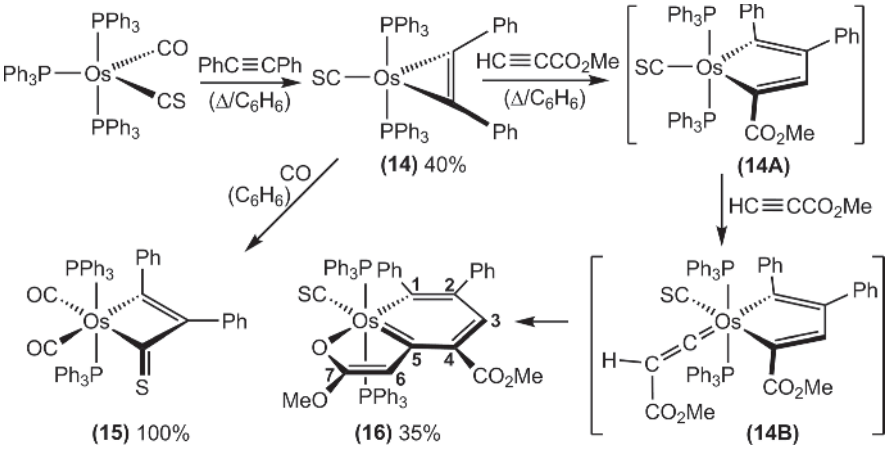

Scheme 1.4 Synthesis of the osmabenzofuran **16**.

$Os(C_7H_2O\{Ph\text{-}1\}\{Ph\text{-}2\}\{CO_2Me\text{-}4\}\{OMe\text{-}7\})(CS)(PPh_3)_2$ (**16**) in 35% isolated yield after chromatography (Scheme 1.4) [38]. Surprisingly, the CS ligand remained intact and was not incorporated into either of the two fused rings. It was proposed that the reaction proceeds via cyclisation of the diphenyl acetylene with a coordinated methyl propiolate to give the intermediate osmacyclopentadiene **14A**. This does not then undergo a migratory insertion reaction with the adjacent CS. Instead an additional methyl propiolate coordinates and rearranges into a vinylidene ligand to give intermediate **14B** (Scheme 1.4). It is well known that coordinated methyl propiolate can rearrange to a vinylidene ligand ($M=C=CR_2$) [39–41]. After insertion of the vinylidene carbon, coordination of the carbonyl oxygen of the ester substituent forms the fused metallafuran ring in **16** [38].

The osmabenzofuran **16** was found to be relatively unreactive and the extensive ring substitution may be, at least in part, responsible for this. It does, however, undergo protonation and on treatment with aqueous hydrochloric acid the colour changes from blue-green to green. The protonation occurs at C6 and this was confirmed by ^1H NMR spectroscopy (Scheme 1.5). The protonation is readily reversed, and if dilute acid is used only unreacted **16** is collected when attempts are made to isolate the protonated species. However, if gaseous HI (contaminated with a small amount of iodine impurity) is added to a dichloromethane solution of **16,** the green cationic tethered osmabenzene $[Os(C_5H\{Ph\text{-}1\}\{Ph\text{-}2\}\{CO_2Me\text{-}4\}\{CH_2C(O)OMe\text{-}5\})(CS)(PPh_3)_2][I_3]$ (**17**) (Scheme 1.5) can be isolated and structurally characterised. Protonation at C6 saturates this carbon atom and this disrupts the π-delocalisation in the five-membered ring. The five-membered ring can then be viewed as a simple "tethering arm" to the osmabenzene. We have used the term "tethering arm" to distinguish this type of fused ring from those that can support delocalised π-systems [38, 42]. As might be expected, treatment of these protonated osmabenzofurans with base instantly returns the original osmabenzofuran **16**.

An illustration of the chemically robust nature of this osmabenzofuran skeleton is provided by the observation that heating **16** under reflux in a benzene/ethanol mixture containing a small amount of concentrated HCl for 1 h results in the formation of the blue-green trans-esterified osmabenzofuran, $Os(C_7H_2O\{Ph\text{-}1\}\{Ph\text{-}2\}\{CO_2Et\text{-}4\}\{OMe\text{-}7\})(CS)(PPh_3)_2$ (**18**), which can be isolated in 51% yield (Scheme 1.5). It is noteworthy that the methyl ester function on the six-membered metallacyclic ring undergoes *trans*-esterification under these conditions, but the methoxy substituent on the five-membered ring remains intact. This suggests that even under these harsh conditions the osmafuran ring is not opened by cleavage of the Os–O bond to give a pendant methyl ester function [38].

The structures of the osmabenzenoids **16–18** have been determined unambiguously by single crystal X-ray crystallographic studies (Figure 1.4). In all cases the osmium

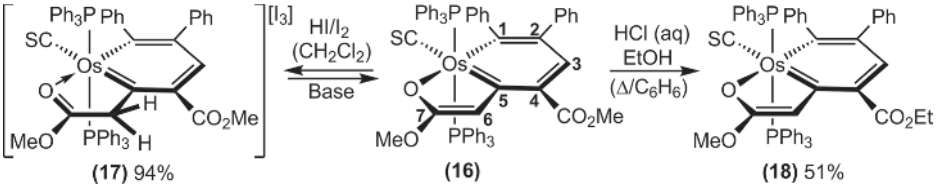

(17) 94% **(16)** **(18)** 51%

Scheme 1.5 Preparation of derivatives of **16**.

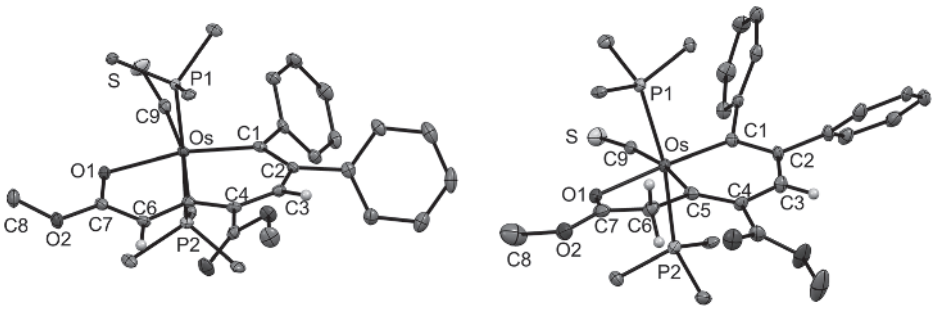

Figure 1.4 Molecular structures of the osmabenzofuran **16** (left) and the cation of the tethered osmabenzene **17** (right) showing 50% probability thermal ellipsoids. Some hydrogen atoms and the phenyl rings of the triphenylphosphine ligands are not shown for clarity. Selected distances [Å] for **16**: Os–C1 2.068(3), Os–C5 2.142(3), Os–O1 2.2178(17), Os–C9 1.846(3), C1–C2 1.376(4), C2–C3 1.442(3), C3–C4 1.359(4), C4–C5 1.436(4), C5–C6 1.371(3), C6–C7 1.416(4), C7–O1 1.250(3). Selected distances [Å] for **17**: Os–C1 1.996(5), Os–C5 2.103(6), Os–O1 2.221(4), Os–C9 1.901(6), C1–C2 1.450(8), C2–C3 1.374(8), C3–C4 1.438(8), C4–C5 1.375(8), C5–C6 1.507(8), C6–C7 1.495(9) C7–O1 1.226(8). (*See color plate section for the color representation of this figure.*)

metal lies at a ring junction position of the two fused rings with the oxygen atom coordinated to osmium. The two fused rings are essentially planar in the osmabenzofurans **15** and **16**. The tethered osmabenzene **17**, on the other hand, displays moderate nonplanarity with the mean deviation from the Os, C1–C7, O1 least-squares plane being 0.14 Å. It is perhaps not surprising that the largest deviation from the mean plane was observed for the saturated atom, C6 (0.25 Å) [38].

In the osmabenzofuran **16**, the osmium–carbon bond lengths (Os–C1 2.068(3), Os–C5 2.142(3) Å) are similar to those observed in osmabenzenes [14, 25, 43–45], and the longer Os–C5 distance is most likely due to the *trans* influence of the thiocarbonyl ligand. The carbon–carbon bonds in the two rings display some bond length alternation but all fall midway between the expected distances for single and double bonds and are similar to the C–C distances reported for other metallabenzenes. The structure of **18** is essentially the same as **16** except for the presence of the ethyl rather than methyl group [38].

Protonation of C6 in **16** to give the cationic tethered osmabenzene **17** causes a number of significant changes in the structural parameters. The osmium–carbon bond lengths in **17** are notably shorter (Os–C1 1.996(5), Os–C5 2.103(6) Å), and the bonds to C6 are significantly longer (C5–C6 1.507(8), C6–C7 1.495(9) Å) and are consistent with single bonds. The carbon–carbon bond lengths in the six-membered osmabenzene ring are similar to those found in **16** and **18**. The long C5–C6 and C6–C7 distances in particular provide compelling evidence for the "tethered osmabenzene" formulation of **17** [38].

In the infrared spectrum of **16**, a strong absorbance at 1229 cm^{-1} is assigned to the thiocarbonyl ligand and the two bands at 1695 and 1569 cm^{-1} are assigned to the ester function on C4. Absorbance bands in similar positions are also found in **17** and **18**. The extensive substitution on the osmabenzofuran rings means that there are few signals in the aromatic region of the ^{1}H NMR spectra of these compounds. The H3 protons are found at 6.99, 8.39 and 6.98 ppm in **16**, **17** and **18**, respectively. It is possible that the

lower-field H3 shift for **17** results from the π-system that is now delocalised over only the six atoms of the osmabenzene ring. The single protons on C6 in **16** and **18** are found at 6.51 and 6.49 ppm, respectively, while in the spectrum of the tethered osmabenzene **17**, the two protons on C6 are observed at 2.94 ppm. The large up-field shift is consistent with saturation of C6 and the loss of π-delocalisation in the furan ring. There are significant differences between the ^{13}C NMR spectra of **16** and **17**. For **16**, C1 and C5 are observed at 196.4 and 218.9 ppm, respectively, suggesting multiple bond character in each of the Os–C1 and Os–C5 bonds. The remaining carbon atoms of the two fused rings are found in typical aromatic positions (137.6 (C2), 158.1 (C3), 124.4 (C4), 123.6 (C6), 184.7 (C7) ppm) and are consistent with significant delocalised bonding in the two fused rings. In the ^{13}C NMR spectra of **17**, C1 and C5 are observed at considerably lower field positions (279.2 and 243.5 ppm, respectively), which may suggest increased multiple bonding to osmium with π-delocalisation now only over the six-membered ring. The remaining osmabenzene ring carbon atoms appear in the normal aromatic range (148.3 (C2), 153.8 (C3), 135.7 (C4) ppm). Carbon C6 in **17** is saturated, and accordingly is found in the up-field position of 52.7 ppm. In summary, the combination of the spectral and structural data corroborates the osmabenzene description for this complex [38].

1.3.2 Ruthenabenzofurans

Preparation of the osmabenzofuran complexes focused our attention on the possibility that metallabenzofurans involving other metals can also be prepared. On searching the literature we found that a ruthenium compound which fulfilled the criterion to be considered a ruthenabenzofuran had already been reported (complex **19**; Scheme 1.6), although at the time it was not recognised as such [46, 47]. With the benefit of the knowledge we had obtained from our studies of the osmabenzofurans **16** and **18**, it became clear to us that this alternative formulation was appropriate [42]. The ruthenabenzofuran $Ru(C_7H_3O\{CO_2Me\text{-}2\}\{CO_2Me\text{-}4\}\{OMe\text{-}7\})(CO)(PPh_3)_2$ (**19**) had been prepared by treatment of the ruthenium complex $RuH_2(CO)(PPh_3)_2$ with methyl propiolate in refluxing benzene (Scheme 1.6) [46]. Three molecules of methyl propiolate cyclised at the ruthenium metal centre to form the red-violet product. It was proposed that the

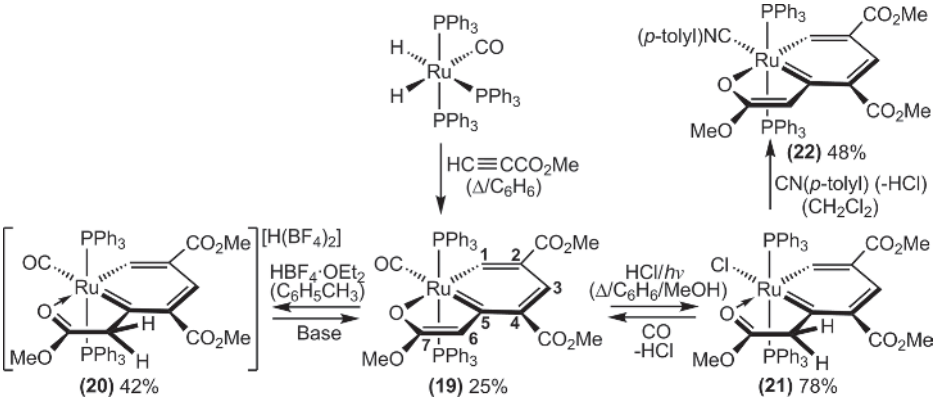

Scheme 1.6 Syntheses of the ruthenabenzene **19** and its derivatives.

mechanism of this reaction first involved the cyclisation of two molecules of methyl propiolate at the ruthenium centre to form a ruthenacyclopentadiene intermediate. A third methyl propiolate then rearranged at the metal centre to form a coordinated vinylidene ligand, the α-carbon atom of which then inserted into an Ru–C bond of the ruthenacyclopentadiene. Coordination of the carbonyl oxygen of the ester function from the vinylidene ligand then formed the fused ruthenafuran ring and at the same time aromatised the six-membered ring, thereby forming the ruthenabenzofuran.

Since we had shown that the furan carbon atom C6 of the osmabenzofuran **16** was susceptible to protonation, the reactivity of ruthenabenzofuran **19** towards acids was investigated. Indeed, it was found that on addition of the anhydrous acid $HBF_4{\cdot}OEt_2$ to a solution of **19** in toluene, protonation at C6 occurred immediately and the dark blue $[Ru(C_5H_2\{CO_2Me\text{-}2\}\{CO_2Me\text{-}4\}\{CH_2C(O)OMe\text{-}5\})(CO)(PPh_3)_2][H(BF_4)_2]$ (**20**) precipitated from solution in 42% isolated yield (Scheme 1.6). The two protons on the saturated carbon atom C6 are observed in the ^{1}H NMR spectrum at 2.73 ppm. This tethered ruthenabenzene complex, which has been structurally characterised, is stable for several days in solution at ambient temperature. However, on the addition of bases such as triethylamine, the protonation reaction is easily reversed and **19** is returned in excellent yield [42].

A related neutral tethered ruthenabenzene can be obtained if very different reaction conditions are employed. Treatment of a refluxing benzene/methanol solution of the ruthenabenzofuran **19** with trimethylsilyl chloride (which acts as a source of anhydrous hydrochloric acid) while simultaneously irradiating with visible light (to accelerate CO dissociation) over a period of 3–4 h gives the green, tethered ruthenabenzene, $Ru(C_5H_2\{CO_2Me\text{-}2\}\{CO_2Me\text{-}4\}\{CH_2C(O)OMe\text{-}5\})Cl(PPh_3)_2$ (**21**), in 78% yield after purification by column chromatography. Under these conditions C6 is protonated and the carbonyl ligand is replaced by chloride. The two protons on the saturated carbon atom C6 are observed in the ^{1}H NMR spectrum at 3.19 ppm. The stability of **19** in the presence of HCl, while being irradiated and heated under reflux for hours in a benzene/methanol solution, is remarkable. Although only a few ruthenabenzenes have been reported, it is interesting to note that in some cases they are thermally unstable [48], while other examples show unexpectedly high thermal stability [49–51]. The tethered ruthenabenzene **21** is very stable in solutions containing traces of HCl, but on the addition of bases intractable mixtures of products are formed. Treatment of a dichloromethane solution of **21** with carbon monoxide, on the other hand, results in the replacement of chloride by CO, proton loss from C6 and reformation of the ruthenabenzofuran **19** in good yield. Treatment of **21** with the isoelectronic *p*-tolylisocyanide (CN{*p*-tolyl}) proceeds in a similar manner to give the new ruthenabenzofuran, $Ru(C_7H_3\{CO_2Me\text{-}2\}\{CO_2Me\text{-}4\}\{OMe\text{-}7\})(CN(p\text{-}tolyl))(PPh_3)_2$ (**22**) (Scheme 1.6), which is the *p*-tolylisocyanide analogue of **19** [42].

The NMR spectral data have been reported for the ruthenabenzofurans **19** and **22**, as well as the related tethered ruthenabenzenes **20** and **21**. In addition, the molecular structures of **19**, **20** and **21** have been obtained. This enables useful comparisons to be made between the properties of these ruthenabenzofurans and the closely related tethered ruthenabenzenes.

In the ^{1}H NMR spectra of the ruthenabenzofurans **19** and **22**, the fused ring protons unsurprisingly appear in similar positions (**19** 11.67 (H1), 7.2–7.5 (H3 obscured by PPh_3 multiplet), 6.06 (H6) ppm [47]; **22** 12.40 (H1), 7.3–7.4 (H3 obscured by PPh_3),

6.17 (H6) ppm). However, the corresponding signals for the metallabenzene ring protons of the related tethered ruthenabenzenes **20** and **21** are both observed at considerably lower-field positions (**20** 14.97 (H1), 8.83 (H3) ppm; **21** 16.45 (H1), 8.76 (H3) ppm) [42]. A similar trend is observed for the chemical shifts of the ring carbon atoms in the ^{13}C NMR spectra. Thus, the signals for the metal-bound carbon atoms C1 and C5 in the tethered ruthenabenzenes **20** and **21** are observed at significantly lower field positions (**20** 290.8 (C1) and 283.6 (C5) ppm, **21** 289.3 (C1) and 287.8 (C5) ppm) than the resonances for the corresponding carbon atoms in the related ruthenabenzofurans **19** and **22** (**19** 232.9 (C1) and 227.0 (C5) ppm, **22** 245.0 (C1) and 232.8 (C5) ppm) [42]. Shifts of the Cα and Hα resonances to lower field values is consistent with increasing π-bonding between the metal and Cα in these closely related compounds and hence may signal increased π-delocalisation over the six-membered metallacyclic rings in the tethered ruthenabenzenes in comparison to the ruthenabenzofurans [22].

There are also some interesting differences in the structural parameters associated with the six-membered metallacyclic rings of the ruthenabenzofurans **19** and **22** compared to those of the tethered ruthenabenzene **20** (Figure 1.5) [42, 46, 47]. While these rings are essentially planar in all three compounds, the Ru–C distances in the tethered ruthenabenzene **20** (Ru–C1 1.933(4), Ru–C5 2.045(5) Å) are significantly shorter than those in the ruthenabenzofurans **19** (Ru–C1 2.004(6), Ru–C5 2.093(5) Å) and **22** (Ru–C1 1.986(3), Ru–C5 2.092(4) Å). In addition, the range of metallabenzene ring C–C distances in **20** show a smaller spread (1.374(7)–1.413(7) Å) compared to the ranges in **19** (1.338(9)–1.450(10) Å) and **22** (1.368(5)–1.475(5) Å). These structural features are also consistent with greater aromatic character for the six-membered metallacyclic ring of the tethered ruthenabenzene **20** compared to the ruthenabenzofurans **19** and **22**.

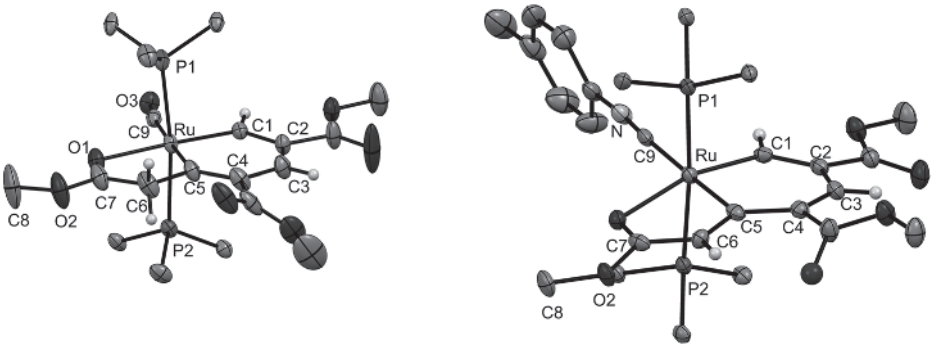

Figure 1.5 Molecular structures of the cation of the tethered ruthenabenzene **20** (left) and the ruthenabenzofuran **22** (right) showing 50% probability thermal ellipsoids. The phenyl rings of the triphenylphosphine ligands and most hydrogen atoms are not shown for clarity. Selected distances [Å] for **20**: Ru–C1 1.933(4), Ru–C5 2.045(5), Ru–O1 2.216(3), Ru–C9 1.941(5), C1–C2 1.404(6), C2–C3 1.383(7), C3–C4 1.413(7), C4–C5 1.374(7), C5–C6 1.518(7), C6–C7 1.504(8), C7–O1 1.231(7). Selected distances [Å] for **22**: Ru–C1 1.986(3), Ru–C5 2.092(4), Ru–O1 2.266(2), Ru–C9 1.954(4), C1–C2 1.368(5), C2–C3 1.437(5), C3–C4 1.376(5), C4–C5 1.475(5), C5–C6 1.376(5), C6–C7 1.437(5), C7–O1 1.242(4).

1.3.3 Iridabenzofurans

The successful isolation of osmabenzofuran and ruthenabenzofuran derivatives led us to consider the synthesis of the related iridabenzofurans. The mechanisms proposed for the formation of the group 8 metallabenzofurans involved, in the last steps, the insertion of a vinylidene ligand (formed by the rearrangement of a coordinated methyl propiolate) into preformed (but not isolated or detected) metallacyclopentadiene intermediates. Since the stable, isolated iridacyclopentadiene $[Ir(C_4H_4)(CO)(NCMe)(PPh_3)_2][O_3SCF_3]$ (**23**) (see Scheme 1.7) was known, it seemed logical that we should investigate the reaction of this compound with methyl propiolate [28]. Attractive features of **23** were that it could be synthesised easily and in high yield through reaction between the iridium(I) cation, $[Ir(NCMe)(CO)(PPh_3)_2][OTf]$, and ethyne, and that the relatively labile acetonitrile ligand should facilitate coordination of the alkyne.

Naturally we were delighted to find that when a mixture of iridacyclopentadiene **23** and an excess of methyl propiolate was heated under reflux in 1, 2-dichloroethane, the bright orange cationic iridabenzofuran $[Ir(C_7H_5O\{OMe\text{-}7\})(CO)(PPh_3)_2][OTf]$ (**24**) (Scheme 1.7) was formed in 88% isolated yield. It seems likely that the mechanism does indeed proceed via the intermediate vinylidene complex **23A**, which undergoes migratory insertion of Cα into the iridacyclopentadiene ring. Coordination of the ester carbonyl oxygen atom to iridium then forms the iridafuran ring. The neutral iridabenzofuran derivative $Ir(C_7H_5O\{OMe\text{-}7\})Cl(PPh_3)_2$ (**25**) may be formed by treating **24** with lithium chloride in refluxing *n*-propanol for several hours. Isolation of the bright red crystalline **25** in very good yield following these reaction conditions is a testament to the stability of the iridabenzofurans **24** and **25** [52].

One of the remarkable features of the iridabenzofurans **24** and **25** is the near absence of substituents on the fused rings. In each case there is only a methoxy substituent at C7 on the iridafuran ring. In all previously reported metallabenzofurans the metallacyclic rings had been quite heavily substituted. This minimal ring substitution, coupled with the high-yielding syntheses of **24** and **25**, paved the way for extended studies of the

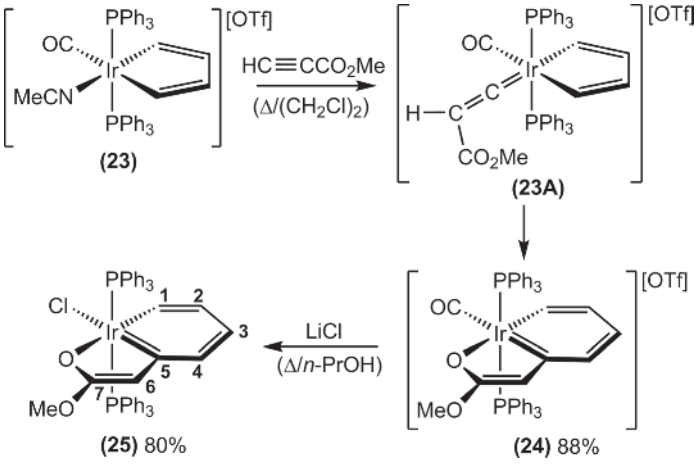

Scheme 1.7 Synthesis of the iridabenzofurans **24** and **25**.

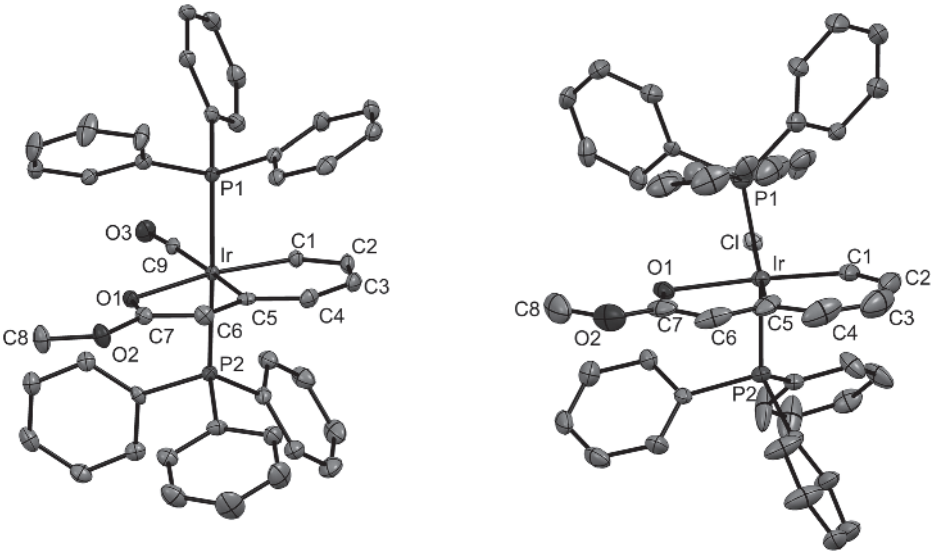

Figure 1.6 Molecular structures of the iridabenzofurans **24** (left) and **25** (right) showing 50% probability thermal ellipsoids. Hydrogen atoms and the counter anion of **24** are not shown for clarity. Selected distances [Å] for **24**: Ir–C1 2.049(3), Ir–C5 2.073(2), Ir–O1 2.2152(19), Ir–C9 1.946(2), C1–C2 1.358(4), C2–C3 1.455(4), C3–C4 1.353(4), C4–C5 1.441(3), C5–C6 1.382(3), C6–C7 1.435(3), C7–O1 1.265(3). Selected distances [Å] for **25**: Ir–C1 1.998(5), Ir–C5 1.987(6), Ir–O1 2.256(3), Ir–Cl 2.4682(13), C1–C2 1.337(7), C2–C3 1.425(9), C3–C4 1.360(9), C4–C5 1.444(8), C5–C6 1.385(8), C6–C7 1.403(8), C7–O1 1.267(6).

reaction chemistry of these species. This was to provide some valuable insights into the chemistry of metallabenzofurans, and this is discussed in Section 1.4.1.

The molecular structures of the iridabenzofurans **24** and **25** were obtained (see Figure 1.6) [52]. In each case the overall geometry about the iridium centre is approximately octahedral with iridium occupying a ring junction position of the essentially planar fused rings. The CO or Cl ligands complete the equatorial plane and the two mutually *trans* triphenylphosphine ligands occupy the axial positions. The iridium–carbon distances in cationic iridabenzofuran **24** (Ir–C1 2.049(3), Ir–C5 2.073(2) Å) are significantly longer than in the neutral derivative **25** (Ir–C1 1.998(5), Ir–C5 1.987(6) Å) but are still within the range of metal–carbon bond lengths observed in iridabenzenes [32, 33, 53–57]. These distances can be compared with the two longer iridium–C(sp^2) single-bond distances found in the cationic iridacyclopentadiene complex $[Ir(C_4H_4)(CHCHNEt_3)(CO)(PPh_3)_2][ClO_4]$ (2.114(6), and 2.094(6) Å) [58]. There is a degree of carbon–carbon bond length alternation in the fused rings of both the cationic iridabenzofuran **24** (range of C–C distances 1.353(4)–1.455(4) Å) and in the neutral iridabenzofuran **25** (range of C–C distances 1.337(7)–1.444(8) Å) [52].

The minimal ring substitution in these two complexes means that more detailed information can be obtained from the ^{1}H NMR spectra. The chemical shifts of H1 in **24** (7.70 ppm) and **25** (9.36 ppm) are not found as far down-field as they are in typical iridabenzenes (10–14 ppm), but they are further down-field than the protons on the metal-bound carbon atoms in the iridacyclopentadiene complex **23** (6.75 and 7.30 ppm). The

remaining ring protons are observed slightly up-field of typical aromatic compounds (**24** 5.92 (H2), 5.64 (H3), 5.58 (H4), 5.55 (H6) ppm; **25** 5.93 (H2), 5.52 (H3), 4.68 (H4), 4.91 (H6) ppm) [52], and iridabenzenes (6–8 ppm) [34, 59, 60]. Similarly, in the ^{13}C NMR spectra the average chemical shifts of the metal-bound carbon atoms C1 and C5 (**24** 128.20, 197.60 ppm, respectively; **25** 148.61, 193.71 ppm, respectively) [52] are found between those of iridabenzenes (typically 180–250 ppm) [34, 59, 60] and the iridacyclopentadiene **23** (132.00 and 151.84 ppm). The chemical shifts of carbon atoms remote from the iridium are found in characteristic aromatic positions (**24** 123.72 (C2), 140.97 (C3), 125.72 (C4), 121.57 (C6); **25** 121.12 (C2), 141.05 (C3), 121.08 (C4), 114.82 (C6) ppm) [52].

The structural and spectral data are consistent with a π-bonding system that is delocalised over the two fused rings of **24** and **25**. However, the delocalisation over the six-membered metallacyclic rings appears to be less extensive than that in typical iridabenzenes. The data may also point to slightly more delocalisation in neutral **25** than in cationic **24**.

The structural and NMR spectral data collected for all the metallabenzofurans described above suggest that the aromaticity in the primary six-membered metallacyclic ring is somewhat reduced with the addition of a fused furan ring. This would be consistent with the situation for simple organic benzenoids, where computational studies have shown that the aromatic stabilisation energy associated with a six-membered aromatic ring is reduced (compared to benzene) when additional fused rings are present [61].

1.3.4 Iridabenzothiophenes

As is noted above, the cationic iridium(I) thiocarbonyl complex, $[Ir(CS)(NCMe)(PPh_3)_2][OTf]$, reacts with two molecules of ethyne to give the cationic iridacyclopentadiene complex, $[Ir(C_4H_4)(CS)(NCMe)(PPh_3)_2][OTf]$ (**7**) (see Scheme 1.3). During our studies of the reactions of alkynes with iridium thiocarbonyl complexes, we found that the neutral analogue, $IrI(CS)(PPh_3)_2$, also undergoes reaction with two molecules of ethyne if more vigorous conditions such as heating under reflux in benzene are employed. However, in this case a very different product, $Ir(C_3H_2\{SCHCH\text{-}1\})I(PPh_3)_2$ (**26a**) (Scheme 1.8), is formed. This complex can be viewed as an iridacyclobutadiene with a fused iridathiophene ring. If phenylacetylene or methyl propiolate are used in place of ethyne, the analogous compounds $Ir(C_3H\{SCPhCH\text{-}1\}\{Ph\text{-}3\})I(PPh_3)_2$ (**26b**) or $Ir(C_3H\{SC[CO_2Me]CH\text{-}1\}\{CO_2Me\text{-}2\})I(PPh_3)_2$ (**27**), respectively, are obtained [62].

The iridium centre of the fused-ring iridacyclobutadiene **27** is coordinatively saturated and relatively inert to further insertion of alkynes, most likely due to the tightly bound ancillary ligands. However, it was found that if silver triflate is added to **27** the iodide ligand is precipitated as silver iodide. This opens up access to the metal centre, and on addition of methyl propiolate to the resulting intermediate cationic complex both carbon atoms of the alkyne insert into the iridium–carbon bond of the iridacyclobutadiene ring to form a fused-ring iridabenzene. After addition of lithium chloride the neutral iridabenzothiophene, $Ir(C_5H_2\{SC[CO_2Me]CH\text{-}1\}\{CO_2Me\text{-}2\}\{CO_2Me\text{-}4\})Cl(PPh_3)_2$ (**28**) (Scheme 1.8), can then be isolated as blue-green crystals in good yield [62].

The structure of **28** reveals that the iridium metal occupies a ring junction position of the fused iridabenzene and iridathiophene rings that is remote from the sulfur atom

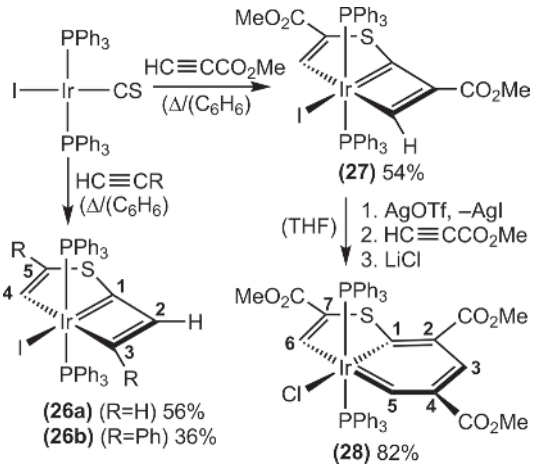

Scheme 1.8 Synthesis of the fused-ring iridacyclobutadienes **26–27** and the iridabenzothiophene **28**.

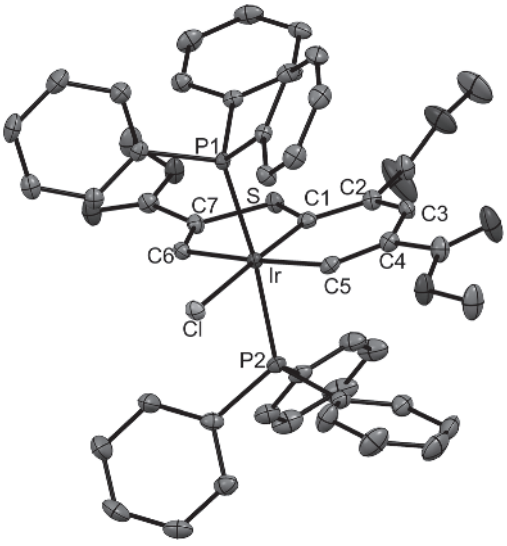

Figure 1.7 Molecular structure of iridabenzothiophene **28** showing 50% probability thermal ellipsoids. Hydrogen atoms are not shown for clarity. Selected distances [Å]: Ir–C1 1.973(3), Ir–C5 2.042(3), Ir–C6 2.106(3), Ir–Cl 2.4685(7), C1–C2 1.449(4), C2–C3 1.361(4), C3–C4 1.434(4), C4–C5 1.360(4), C6–C7 1.341(4), C7–S 1.765(3), S–C1 1.722(3).

(Figure 1.7). The six-membered iridabenzene ring is close to planar and the iridium–carbon bond lengths (Ir–C1 1.973(3), Ir–C5 2.042(3) Å) are similar with distances intermediate between those typical for iridium–carbon single and double bonds. The carbon–carbon bond lengths (C1–C2 1.449(4), C2–C3 1.361(4), C3–C4 1.434(4), C4–C5 1.360(4) Å) are also intermediate in length between those of single and double bonds and show significant bond length alternation, which suggests that the valence bond

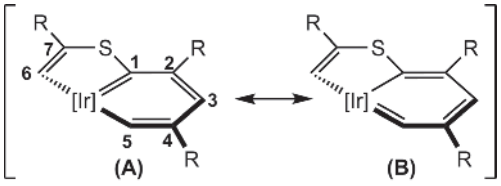

([Ir] = IrCl(PPh$_3$)$_2$, R = CO$_2$Me)

Chart 1.3 Two important valence bond structures of iridabenzothiophene **28**.

structure **A** is more important than **B** (Chart 1.3). Within the five-membered iridathiophene ring, the iridium–carbon bond length, at 2.106(3) Å, is close to an iridium–carbon single bond length, while the carbon–carbon bond length of 1.341(4) Å is more appropriate for a carbon–carbon double bond [62].

The chemical shifts of the iridabenzene carbon and hydrogen atoms in **28** are similar to those reported for other iridabenzenes. The resonance for H5 is observed down-field at 13.25 ppm in the ^{1}H NMR spectrum as a sharp doublet due to a four-bond coupling to proton H3, which is found at 7.63 ppm. The resonances of the metal-bound carbon atoms C1 and C5 are both found significantly down-field (252.7 and 247.5 ppm, respectively) in the ^{13}C NMR spectrum, while the other three ring carbons have typically aromatic chemical shifts (124.0 (C2), 162.0 (C3), 126.8 (C4) ppm). In all cases these chemical shifts fall within the range observed for other iridabenzenes. Within the fused five-membered ring, H6 is found at 10.70 ppm in the ^{1}H NMR spectrum and carbons C6 and C7 at 198.2 and 143.7 ppm, respectively in the ^{13}C NMR spectrum [62]. These resonances are observed somewhat further down-field than would have been expected for a localised bonding situation within the five-membered ring. It is noteworthy that in the ^{13}C NMR spectrum the chemical shifts of the metal-bound carbon atoms of the six-membered metallacyclic ring of **28** are observed further down-field compared to those of the related iridabenzofurans **24** and **25**. Similarly, in the ^{1}H NMR spectrum of **28**, H5 is also found further down-field. These observations may indicate that there is more extensive π-delocalisation in the iridafuran rings of **24** and **25** compared with the iridathiophene ring of **28**. However, appropriate computational studies will be required to provide further information on this point. Complex **28** remains the only example of a metallabenzothiophene to have been reported.

1.3.5 Iridabenzothiazolium Cations

The preferred route to the iridabenzene Ir(C$_5$H$_4${SMe-1})Cl$_2$(PPh$_3$)$_2$ (**13**) (see Scheme 1.3) involved methylation of the sulfur atom of the intermediate iridabenzene [Ir(C$_5$H$_4${S-1})(NCMe)(PPh$_3$)$_2$][OTf] (**9**) followed by addition of chloride. If triflic acid is added to **9** instead of methyl triflate, the reaction takes a very different course. On treatment of **9** with two equivalents triflic acid (in a dichloromethane solution containing 10 equivalents of acetonitrile), the brown solution immediately turns red. It is proposed that this red intermediate is the thiol-substituted iridabenzene [Ir(C$_5$H$_4${SH-1})(NCMe)$_2$(PPh$_3$)$_2$][OTf]$_2$ (**9A**) (Scheme 1.9). While this intermediate could not be isolated, treatment of the red solution with ammonium hexafluorophosphate (NH$_4$PF$_6$) in ethanol enabled the deep-green iridabenzothiazolium cation, [Ir(C$_5$H$_4${SC[Me]NH-1})(NCMe)(PPh$_3$)$_2$]

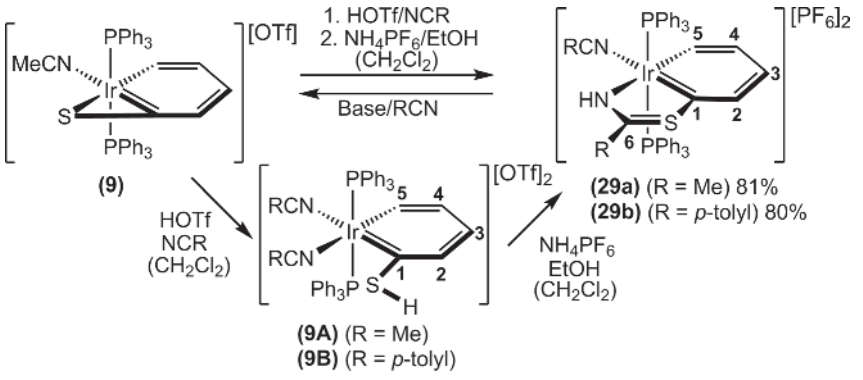

Scheme 1.9 Synthesis of the iridabenzothiazolium cations **29a** and **29b**.

$[PF6]_2$ (**29a**), to be isolated in 81% yield. The analogous complex $[Ir(C_5H_4\{SC[p\text{-tolyl}]NH\text{-}1\})(NC(p\text{-tolyl}))(PPh_3)_2][PF_6]_2$ (**29b**) can be isolated in 80% yield by employing *p*-tolunitrile rather than acetonitrile (Scheme 1.9) [32]. These iridabenzothiazolium cations can be considered the protonated organometallic analogues of benzothiazoles.

While the intermediates **9A** and **9B** could not be isolated as pure solids, they can be detected by NMR spectroscopy. If protected from air, solutions of the red intermediates generated in situ are stable for days. The ^{1}H NMR spectrum of the intermediate metallabenzenethiol **9A** reveals signals at 11.50 (H5), 7.23 (SH), 7.04 (H4), 6.90 (H3), and 6.89 (H2) ppm, each integrating for one proton, in addition to two singlets integrating for three protons at 2.02 and 2.03 ppm, which correspond to the methyl groups of the two acetonitrile ligands. The structure proposed for intermediate **9A** is essentially the same as that of the iridabenzene $[Ir(C_5H_4\{SMe\text{-}1\})(NCMe)_2(PPh_3)_2][PF_6]_2$ (**11**) (Scheme 1.3) except that the sulfur is protonated rather than methylated. Indeed, the ^{1}H NMR spectra of **9A** and **11** are very similar. Addition of excess ethanol to the red solution of **9A** causes a swift colour change to deep green and the NMR signals confirm the formation of the iridabenzothiazolium **29a**. Addition of ammonium hexafluorophosphate enables **29a** to be isolated as the crystalline hexafluorophosphate salt. The addition of water instead of ethanol also brought about this conversion. It is not clear exactly what part ethanol or water plays in the conversion of **9A**/**B** to **29a**/**b**, but it is possible these solvents facilitate proton transfer from sulfur to nitrogen [32].

The crystal structure of **29b** has been obtained and the molecular geometry of the iridabenzothiazolium cation is shown in Figure 1.8. The iridium has an approximately octahedral geometry and the two fused rings are nearly planar, with the maximum deviation from the Ir, C1–C6, S, N least squares plane being 0.064(3) Å for nitrogen. The iridium metal lies at a ring junction position, bound to the nitrogen of the fused five-membered ring. The metal–carbon and carbon–carbon bond lengths in the six-membered metallacyclic ring are similar to those observed in other iridabenzenes and do not exhibit any unusual C–C bond length alternation. The carbon–sulfur bond lengths (C1–S 1.754(5), S–C6 1.757(5) Å) and the carbon–nitrogen bond length (1.290(6) Å) are consistent with limited delocalised π-bonding in the five-membered ring and are similar to those reported for organic benzothiazolium ions [32].

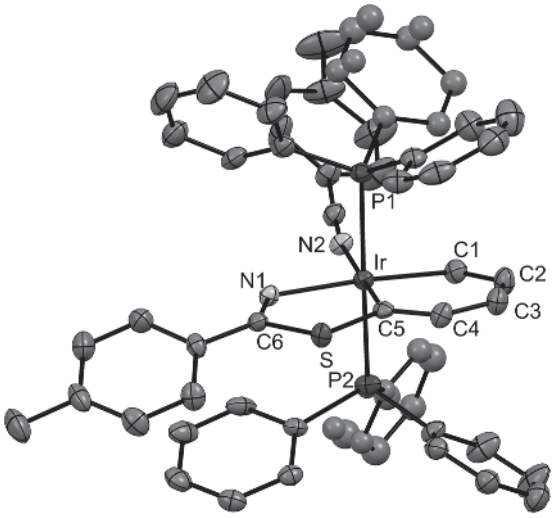

Figure 1.8 Molecular structures of the cation of **29b** showing 50% probability thermal ellipsoids. Hydrogen atoms are not shown for clarity. Selected distances [Å]: Ir–C1 1.953(5), Ir–C5 2.009(5), Ir–N1 2.127(4), Ir–N2 2.093(4), C1–C2 1.396(7), C2–C3 1.385(7), C3–C4 1.402(7), C4–C5 1.360(7), C1–S 1.754(5), S–C6 1.757(5), C6–N1 1.290(6).

The NMR spectra of the two complexes **29a** and **29b** reveal that the π-delocalisation about the six-membered ring is not significantly affected by the addition of the fused thiazolium ring. The aromatic protons in the ^{1}H NMR spectra of **29a** (12.35 (H5), 6.75 (H4), 6.55 (H3), 6.86 (H2) ppm) and **29b** (12.87 (H5), 7.22 (H4), 6.65 (H3), 6.91 (H2) ppm) do not differ significantly from the starting iridabenzene **9**. The NH protons are observed as broad singlets at 10.23 and 10.36 ppm for **29a** and **29b**, respectively, and in the IR spectra the NH groups give rise to broad absorbance bands at 3289 and 3291 cm^{-1} **29a** and **29b**, respectively. Similarly, ^{13}C NMR chemical shifts of the carbon atoms of the iridabenzene rings of **29a** (232.3 (C1), 125.5 (C2), 170.2 (C3), 127.2 (C4), 210.9 (C5) ppm) and **29b** (229.8 (C1), 125.4 (C2), 168.8 (C3), 127.4 (C4), 209.7 (C5) ppm) are typical for iridabenzenes. The resonances for C6 of the thiazolium rings are found at 190.0 ppm in **29a** and at 185.6 ppm in **29b**, each shifted considerably down-field compared to the same carbon atoms in the coordinated ligands prior to annulation [32].

On the basis of the spectroscopic and structural data, the two most important valence bond structures for the fused rings of **29a**/**b** are given in Chart 1.4. The data suggest there is limited π-delocalisation in the fused five-membered rings.

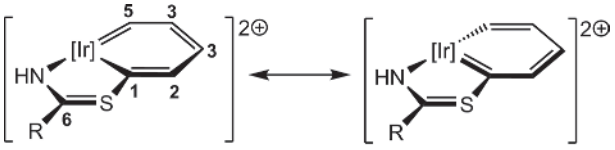

([Ir] = Ir(NCR)(PPh$_3$)$_2$, R = Me or *p*-tolyl)

Chart 1.4 Valence bond structures of metallabenzothiazolium cations.

1.4 Reactions of Metallabenzenes and Metallabenzenoids

In addition to developing new synthetic routes to metallabenzenes and studying the spectroscopic and structural features of these unusual compounds, we were also very interested in the chemical reactivity they exhibited. In this respect we were particularly interested in the similarities and differences between metallabenzenes and the organic congeners, the benzenes. Some of the synthetic routes we had developed enabled us to obtain in moderate to very good yields osmabenzenes, iridabenzenes or iridabenzofurans that had only one ring substituent [22, 27, 34]. This placed us in an excellent position to explore the reaction chemistry of these compounds and this became an increasingly important focus of our research.

1.4.1 Electrophilic Aromatic Substitution Reactions

When we first began studies of the reaction chemistry of the osmabenzene $Os(C_5H_4\{SMe\text{-}1\})I(CO)(PPh_3)_2$ (**3b**) (Scheme 1.10) in the late 1990s, it was still very much an open question as to whether metallabenzenes were aromatic compounds. Detailed theoretical studies that were to confirm the validity of an aromatic description came much later. At that time, to obtain information about this fundamentally important point, we explored the reactions of **3b** with electrophiles. We found that **3b** underwent electrophilic substitution reactions – the classically defining reactions of aromatic, benzenoid compounds. Furthermore, the substitution appeared to follow the same "substituent directing rules" observed in benzene chemistry with the electrophile in this case adding *para* to the –SMe ring substituent (Scheme 1.10) [63].

We found that the blue osmabenzene **3b** undergoes ring bromination when treated with bromine in the presence of iron powder (which was added to form the catalyst $FeBr_3$ in situ) at 40°C. The substitution of hydrogen for bromine occurs at the C4 position, *para*- to the SMe group, to furnish the dark-green osmabenzene $Os(C_5H_3\{SMe\text{-}1\}\{Br\text{-}4\})I(CO)(PPh_3)_2$ (**30**) (Scheme 1.10). The iodide ancillary ligand of the osmabenzene has some lability under these conditions and a small amount of exchange for bromide takes place during the reaction. To overcome the problem of forming products with mixed halide ligands the reaction mixture was treated first with silver perchlorate to abstract the metal-bound halide and then with sodium iodide to return the iodide ligand to the metal. Pure **30** was then isolated in 45% yield following column chromatography. It is interesting to note that, although the –SMe group is an *ortho*/*para* director in benzene chemistry, no sign of substitution *ortho* to the –SMe group was found in these or any other related reactions we subsequently carried out with other electrophiles [63]. Much later we carried out computational studies to determine which of the ring atoms was electronically the most susceptible towards attack by

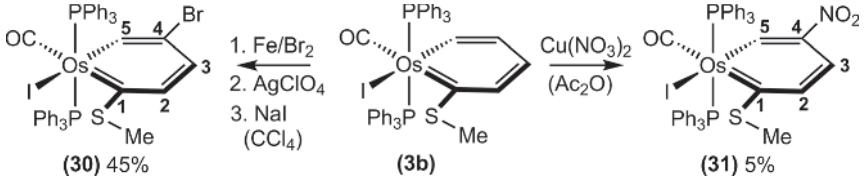

Scheme 1.10 Electrophilic aromatic bromination and nitration reactions of the osmabenzene **3b**.

electrophiles. Indeed, C4 was found to be the preferred site of attack, but this was followed closely by C2 [64]. However, the computational studies did not take into account the influence of steric factors. Presumably our observation of exclusive *para*-substitution is therefore largely a result of the combined steric pressures of the –SMe group and the mutually *trans* PPh_3 ligands in **3b**.

Chlorination occurs at the same ring position, i.e. *trans* to –SMe, and on treatment of **3b** with iodobenzene dichloride ($PhICl_2$) the blue-green product $Os(C_5H_3\{SMe\text{-}1\}\{Cl\text{-}4\})I(CO)(PPh_3)_2$ is formed in 20% yield [63]. Nitration also takes place exclusively at C4 when **3b** is subjected to the fairly mild nitrating conditions of copper nitrate in acetic anhydride (Menke nitration conditions) [65–67]. The mononitroosmabenzene, $Os(C_5H_3\{SMe\text{-}1\}\{NO_2\text{-}4\})I(CO)(PPh_3)_2$ (**31**) (see Scheme 1.13), is isolated in very low yield (5%) as purple crystals following column chromatography [63].

The structural and spectroscopic data indicate the substituted metallabenzene rings in **30** and **31** retain delocalised π-bonding systems. Noteworthy chemical shifts in the ^{1}H NMR spectra include those of the H5 protons, which are found at 12.61 ppm for the brominated **30** and at 14.00 ppm for the nitrated **31** (*cf.* 12.71 ppm in the unsubstituted **3b**). The down-field chemical shift in **31** arises due to the neighbouring strongly electron-withdrawing nitro group, which is also responsible for the down-field shift of proton H3 (to 7.95 ppm in **31** vs. 6.96 ppm in **3b**) and for carbon C4 in the ^{13}C NMR spectrum of **31** (144.24 ppm *cf.* 123.82 ppm in **3b**). The bromo-substituent in **30**, on the other hand, has far less influence on the chemical shifts of the surrounding atoms, with the only significant difference being an up-field shift to 110.56 ppm for carbon C4. The magnitude and direction of all these shifts are similar to those observed in substituted benzenes. The remaining proton and carbon atoms resonate in positions very similar to the corresponding atoms in the starting osmabenzene **3b**. The crystal structures of **30** and **31** (Figure 1.9) confirm the site of substitution but are otherwise unremarkable compared to other osmabenzenes [63].

We subsequently extended this electrophilic aromatic substitution reaction by bromine to encompass iridabenzenes, osmabenzofurans and iridabenzofurans. We discovered that pyridinium tribromide ($[PyH][Br_3]$) is a convenient solid source of bromine that affords brominated products in good yields and requires minimal purification of the crude products. The purple iridabenzene **13** is exclusively monobrominated with this reagent at the C4 position, the same position (*para* to the –SMe ring substituent) that the closely related osmabenzene is substituted. The dark-purple bromoiridabenzene, $Ir(C_5H_3\{SMe\text{-}1\}\{Br\text{-}4\})Br_2(PPh_3)_2$ (**32**) (see Scheme 1.14), is obtained from this reaction in the remarkably high isolated yield of 87% [33]. The blue osmabenzofuran **16** has only two sites available for ring substitution: C3 in the six-membered iridabenzene ring and C6 of the fused furan ring. The preferred site of bromination was found to be C6, and the heavily substituted osmabenzofuran $Os(C_7HO\{Ph\text{-}1\}\{Ph\text{-}2\}\{CO_2Me\text{-}4\}\{Br\text{-}6\}\{OMe\text{-}7\})(CS)(PPh_3)_2$ (**33**) (Scheme 1.14) could be isolated in good 88% yield as green crystals [38]. No evidence was obtained for bromination at C3 in this compound.

The largely unsubstituted bicyclic ring systems of iridabenzofurans **24** and **25** make them ideal candidates for more in-depth studies of the chemical reactivity of metallabenzofurans. The cationic **24** undergoes exclusive monobromination at the C6 site on the fused furan ring on treatment with pyridinium tribromide to give the substituted iridabenzofuran $[Ir(C_7H_4O\{Br\text{-}6\}\{OMe\text{-}7\})(CO)(PPh_3)_2][OTf]$ (**34**) (Scheme 1.11) as

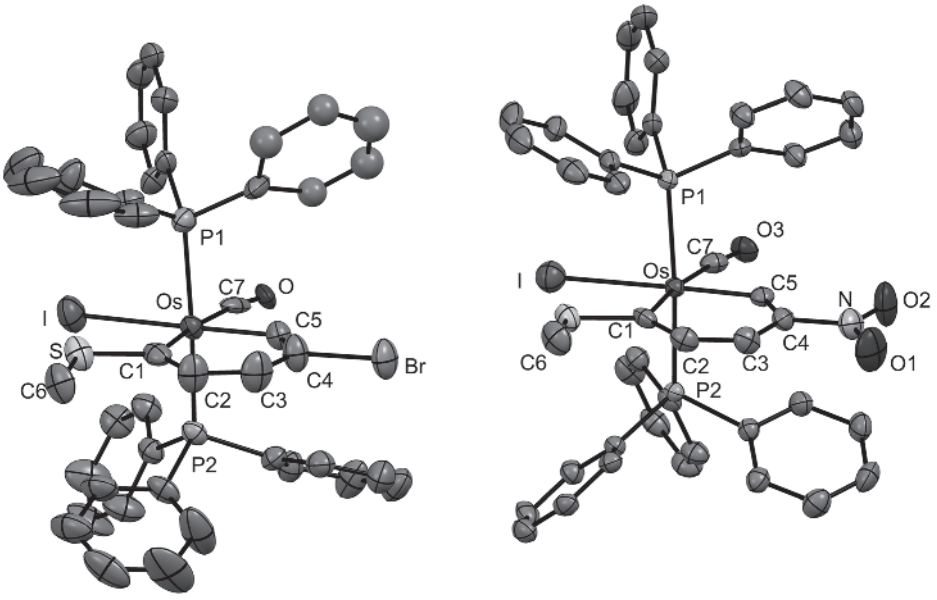

Figure 1.9 Molecular structures of the substituted osmabenzenes **30** (left) and **31** (right) showing 50% probability thermal ellipsoids. Hydrogen atoms are not shown for clarity. Selected distances [Å] for **30**: Os–C1 2.128(9), Os–C5 2.039(9), Os–C7 1.936(13), Os–I 2.8021(9), C1–C2 1.418(13), C2–C3 1.367(14), C3–C4 1.390(14), C4–C5 1.320(13), C1–S 1.702(10), C4–Br 1.968(10). Selected distances [Å] for **31**: Os–C1 2.129(7), Os–C5 2.011(7), Os–C7 1.908(8), Os–I 2.8158(6), C1–C2 1.411(11), C2–C3 1.347(11), C3–C4 1.411(10), C4–C5 1.336(10), C1–S 1.702(7), C4–N 1.476(9). (*See color plate section for the color representation of this figure.*)

red crystals in 70% yield. There was no evidence of further bromination when an excess of the brominating reagent was used, nor was there evidence of any isomers with bromination at a different site. The neutral analogue **25**, however, undergoes exclusive dibromination at C2 and C6 to give the iridabenzofuran $Ir(C_7H_3O\{Br\text{-}2\}\{Br\text{-}6\}\{OMe\text{-}7\})Br(PPh_3)_2$ (**35**) as red crystals in 72% yield. In this case there was no evidence of a mono-substituted product, and even on treatment of **24** with only one equivalent of [PyH][Br_3] a mixture of **35** and unreacted **25** was obtained [52].

In a related electrophilic aromatic substitution reaction, treatment of the iridabenzofuran **25** with mercury trifluoroacetate results in mercuration at the C2, C4 and C6 positions. Following the addition of lithium bromide, the pink trisubstituted iridabenzofuran product $Ir(C_7H_2O\{HgBr\text{-}2\}\{HgBr\text{-}4\}\{HgBr\text{-}6\}\{OMe\text{-}7\})Br(PPh_3)_2$ (**36**) (Scheme 1.12) was isolated in 41% yield. On treatment of **25** with reduced amounts of mercury trifluoroacetate, no mono- or disubstituted products could be isolated. The tri-mercurated compound **36** was the first metallo-substituted metallabenzene derivative to be reported. The carbon–mercury bonds in **36** are easily cleaved on the addition of pyridinium tribromide to give the corresponding tribrominated product $Ir(C_7H_2O\{Br\text{-}2\}\{Br\text{-}4\}\{Br\text{-}6\}\{OMe\text{-}7\})Br(PPh_3)_2$ (**37**) as dark-red crystals in 87% yield [52].

To explain the regioselectivity of all these electrophilic aromatic substitution reactions, a computational study was undertaken. Condensed Fukui functions, derived from DFT calculations, were used as a reactivity index to identify which sites are the

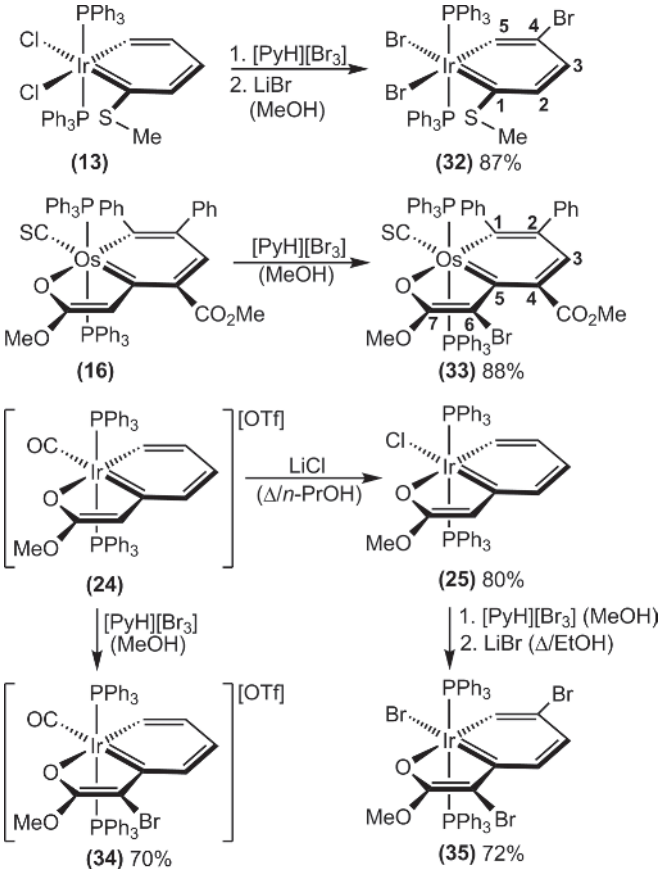

Scheme 1.11 Electrophilic aromatic bromination of the iridabenzene **13**, the osmabenzofuran **16** and the iridabenzofurans **24** and **25**.

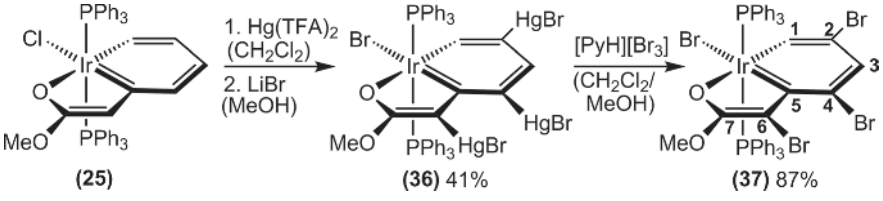

Scheme 1.12 Electrophilic aromatic mercuration of **25** to give the metallo-substituted iridabenzofuran **36** and the cleavage of the C–Hg bonds to give tribrominated iridabenzofuran **37**.

most nucleophilic (i.e. with the largest f_k^- values) and hence the most susceptible to electrophilic attack. It was found that the C1, C2, C4 and C6 sites all possessed large f_k^- values and so electronically these should be the favoured sites for electrophilic substitution. The largest f_k^- value within the fused ring system of the cationic **24** was at C6, consistent with this being the observed site of substitution. The computed f_k^- values for the ring carbons of the monobrominated product **34** are reduced compared

to **24**, which may explain why further bromination of **34** is not observed. For the neutral iridabenzofuran analogue **25**, the most electronically favourable site of substitution is again C6, followed by C4 then C2. In this case bromination at both C2 and C6 is observed. On the other hand, mercuration of **25** yields the tri-mercurated product **36** with substitution occurring at C2, C4 and C6, even though the crystal structure of **36** indicates there is significant steric crowding between the substituents at C4 and C6. While the condensed Fukui functions do correctly indicate the preferred sites for electrophilic attack in these compounds, an important limitation of this approach is that it does not take into account steric factors and this limits its value as a predictive tool [52].

In general, we have found that ring bromination of the metallabenzenes or metallabenzofurans which we have studied has minimal effect on the chemical shifts of the remaining unsubstituted ring carbons and protons in the NMR spectra. In addition, aside from the presence of the bromine substituents, there are only small differences in the structures of the brominated products compared to those of the parent compounds. In the ^{13}C NMR spectra the only significant differences between the brominated products and the parent species is an up-field shift of approximately 10–20 ppm for each carbon atom that bears a bromine substituent. In the bromoiridabenzene **32**, this is carbon C4 (104.78 ppm vs. 121.64 ppm in **13**) [33]. Similar up-field shifts can be observed in the bromoiridabenzofurans **34** (104.36 ppm for C6 vs. 121.57 ppm in **24**), **35** (99.95 ppm for C2, 97.35 ppm for C6) and **37** (101.74, 112.90 and 98.33 ppm for C2, C4 and C6, respectively, vs. 121.12, 121.08 and 114.82 ppm, respectively, in **25**). Analogous up-field shifts are observed upon bromination of simple benzenes. The H1 proton of the trimetallo-substituted **36** is shifted down-field to 10.10 ppm (from 9.36 ppm in **25**) in the ^{1}H NMR spectrum, and proton H3 to 5.90 ppm (from 5.52 ppm in **25**). Further analysis of **36** by ^{13}C NMR spectroscopy could not be made due to the very low solubility of this species [52].

The molecular structures of the brominated derivatives **34** and **35** are shown in Figure 1.10, and the structures of the trisubstituted derivatives **36** and **37** are shown in Figure 1.11. The structural parameters associated with the fused rings show only relatively small changes compared to the corresponding parent compounds **24** and **25**. In all cases the structures are consistent with maintenance of the delocalised π-system over the fused rings.

Electrophilic substitution reactions of the iridabenzofurans **24** and **25** have been extended to nitration. Although only very low yields of the corresponding nitroosmabenzene were obtained from **3b**, much higher yields of nitro-substituted iridabenzofurans were obtained from **24** and **25**. On treatment of the cationic iridabenzofuran **24** with copper nitrate in acetic anhydride at 0°C [65–67], substitution occurs only once and exclusively at C2 to give the nitroiridabenzofuran, $[Ir(C_7H_4O\{NO_2\text{-}2\}\{OMe\text{-}7\})(CO)(PPh_3)_2][OTf]$ (**38**) (Scheme 1.13). This product can be isolated in 52% yield as dark orange crystals. There was no evidence of other isomers or further substitution [68]. The regioselectivity of this reaction was initially quite surprising as in the earlier bromination reactions mono-substitution was found to occur exclusively at the C6 position, and the condensed Fukui functions had indicated that C6 was the most favourable site for attack by electrophiles [52]. However,

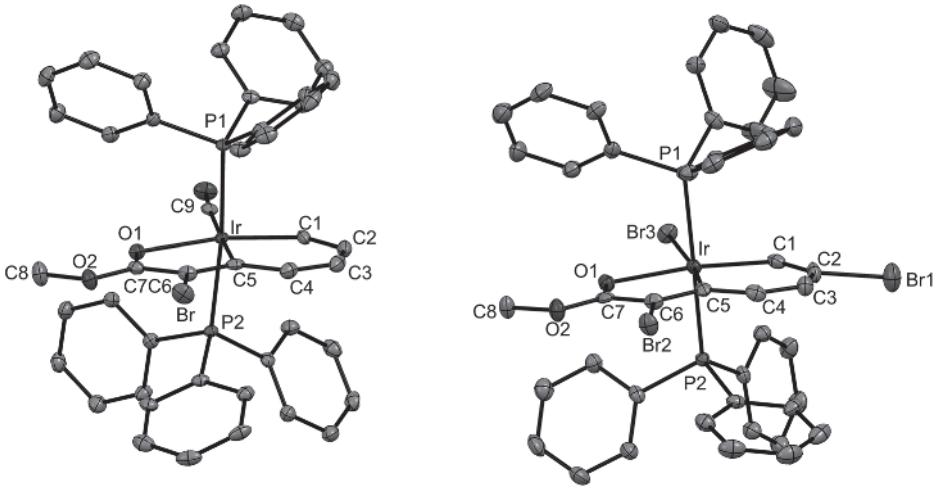

Figure 1.10 Molecular structures of the cation of bromoiridabenzofuran **34** (left) and **35** (right) showing 50% probability thermal ellipsoids. Hydrogen atoms are not shown for clarity. Selected distances [Å] for **34**: Ir–C1 2.019(3), Ir–C5 2.080(3), Ir–O1 2.188(2). Ir-C9 1.948(3), C1-C2 1.350(5), C2-C3 1.451(5), C3-C4 1.350(5), C4-C5 1.443(4), C5-C6 1.353(5), C6-C7 1.445(4), C7-O1 1.261(4), C6-Br 1.909(3). Selected distances [Å] for **35**: Ir-C1 2.023(5), Ir-C5 2.017(5), Ir-O1 2.221(4), Ir-Br3 2.5978(6), C1-C2 1.331(8), C2-C3 1.439(8), C3-C4 1.340(8), C4-C5 1.451(7), C5-C6 1.378(7), C6-C7 1.437(8), C7-O1 1.262(7), C2-Br1 1.948(5), C6-Br2 1.899(5).

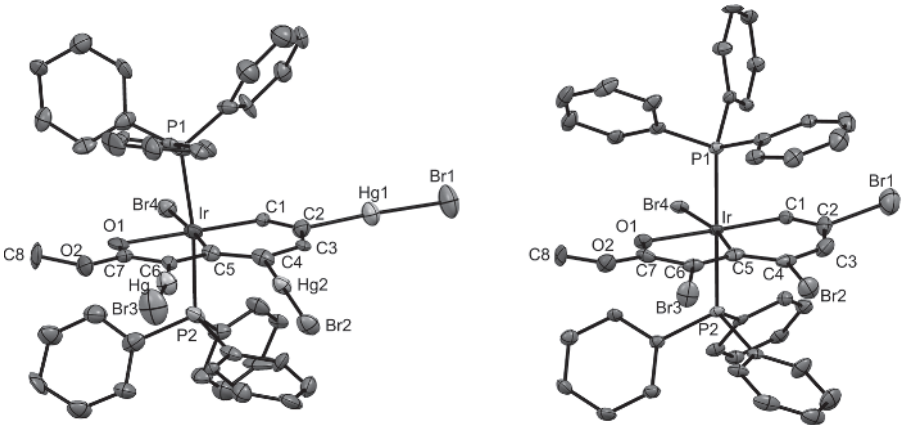

Figure 1.11 Molecular structures of the trisubstituted iridabenzofurans **36** (left) and **37** (right) showing 50% probability thermal ellipsoids. Hydrogen atoms are not shown for clarity. Selected distances [Å] for **36**: Ir–C1 1.99(2), Ir–C5 2.04(2), Ir–O1 2.231(17). Ir-Br4 2.574(3), C1-C2 1.30(3), C2-C3 1.39(3), C3-C4 1.38(3), C4-C5 1.47(3), C5-C6 1.42(3), C6-C7 1.39(3), C7-O1 1.27(3), C2-Hg1 2.13(2), C4-Hg2 2.07(3), C6-Hg3 2.01(2), Hg1-Br1 2.442(3), Hg2-Br2 2.455(3), Hg3-Br3 2.419(3). Selected distances [Å] for **37**: Ir-C1 2.006(8), Ir-C5 2.035(8), Ir-O1 2.159(6), Ir-Br4 2.5746(8), C1-C2 1.306(13), C2-C3 1.397(14), C3-C4 1.352(14), C4-C5 1.453(13), C5-C6 1.369(13), C6-C7 1.450(13), C7-O1 1.243(11), C2-Br1 1.996(9), C4-Br2 1.928(9), C6-Br3 1.912(9).

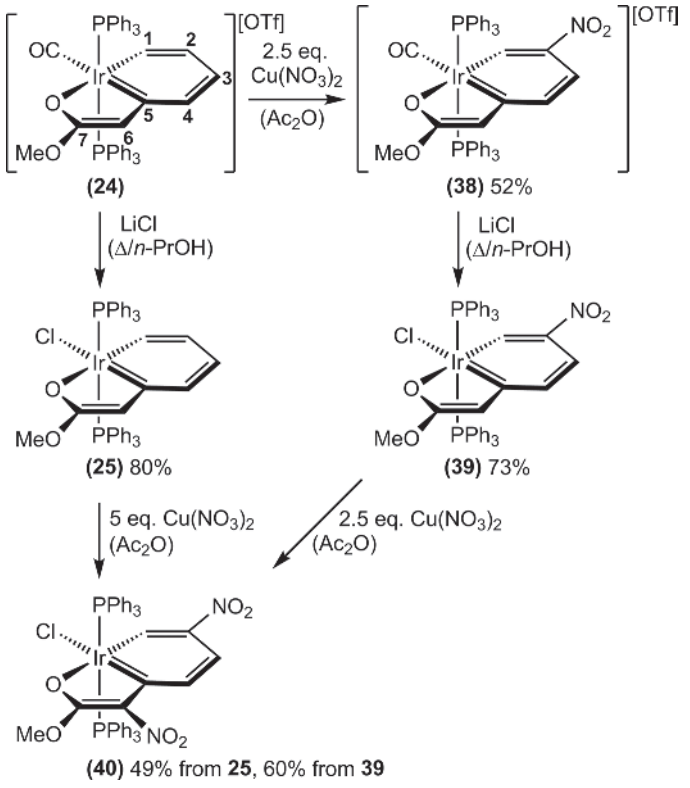

Scheme 1.13 Nitration reactions of the iridabenzofurans **24** and **25**.

it has been reported that nitration of the organic analogue, 2-methylbenzo[*b*]furan, with nitric acid in the presence of tin(IV) chloride gives predominantly 2-methyl-6-nitrobenzo[*b*]furan (which corresponds to nitration at the C2 position of the iridabenzofuran **24**) in addition to lesser amounts of 2-methyl-3-nitrobenzo[*b*]furan (which corresponds to nitration at the C6 position of the iridabenzofuran **24**), with the ratio of these two products being *ca*. 4:1 [69]. In practice, it has been found that the regioselectivity of the nitration of simple benzo[*b*]furans is highly dependent on the nature and position of the substituents on the fused rings, as well as the nitrating reagent employed [70]. Clearly there are a number of subtle but important effects that determine the preferred position of substitution in these nitration reactions. Again, while the f_k^- data successfully indicates the atoms that are susceptible to electrophilic attack in these iridabenzofurans, the method does not enable distinctions to be made reliably between all the potential sites of attack [52, 64].

The neutral analogue **25** can also be nitrated under the same conditions, but in this case the reaction favours disubstitution (at C2 and C6), furnishing the dinitroiridabenzofuran, $Ir(C_7H_3O\{NO_2\text{-}2\}\{NO_2\text{-}6\}\{OMe\text{-}7\})Cl(PPh_3)_2$ (**40**) (Scheme 1.13). When less than two equivalents of copper nitrate are used, some mononitroiridabenzofuran, $Ir(C_7H_4O\{NO_2\text{-}2\}\{OMe\text{-}7\})Cl(PPh_3)_2$ (**39**) can also be isolated from the crude product. However, in

practice it is best to prepare this compound by substitution of the carbonyl ligand in **38** with chloride. Subjecting **39** to the same nitrating conditions also furnishes the dinitrated **40**, although of course this is a less convenient route to this compound. The fact that no C6-mononitroiridabenzofuran could be identified as a component of the product mixture when one equivalent of copper nitrate is used suggests that the dinitration reaction proceeds via initial nitration at C2 rather than C6 [68].

In the NMR spectra of **38**, **39** and **40** the electron-withdrawing nitro group causes deshielding of all nearby proton and carbon atoms, giving rise to down-field chemical shifts compared to the related unsubstituted species. In the ^{13}C NMR spectra, the nitro-bearing carbon C2 is found at 144.14, 143.44 and 142.49 ppm in **38–40**, respectively, and the nitro-bearing C6 carbon in **40** at 135.50 ppm. These are comparable to the nitro-bearing carbon atom in nitrobenzene (148.16 ppm) [71] and are found approximately 20 ppm down-field of the related carbon atom of the unsubstituted complexes **24** and **25** (*ca*. 120 ppm). The metal-bound C1 carbon atoms are also shifted 10–20 ppm down-field by the neighbouring nitro group to 139.76, 167.23 and 173.58 ppm in **38–40**, respectively. Likewise, the H1 protons resonate at 9.74, 12.08 and 12.36 ppm in the ^{1}H NMR spectra of **38–40**, respectively (compared to 7.70 and 9.36 ppm in the unsubstituted **24** and **25**, respectively). The remaining proton and carbon atoms also experience slight down-field chemical shifts, diminishing with distance from the nitro group(s).

The regioselectivities of these nitration reactions have been confirmed by X-ray crystal structure determinations of **38–40**, and the molecular structures of **38** and **40** are shown in Figure 1.12. In each of the complexes **38–40**, the nitro substituent at C2 is nearly coplanar with the Ir, C1–C7 and O1 least-squares plane. The second nitro substituent on carbon C6 of complex **40** is much more sterically hindered, and is rotated about 42° from the same plane. The metallacyclic rings of each of the nitrated complexes are close to planar, in some cases even more so than in the unsubstituted analgoues, which is consistent with the computational determination that π-electron-withdrawing substituents favour planarity in metallabenzenes [35]. The metal–carbon and carbon–carbon bond lengths are otherwise very similar to other iridabenzofurans.

Another interesting observation that was noted during the studies of the nitration reactions of iridabenzofurans was that when a halide salt was introduced to the copper nitrate-acetic anhydride nitrating mixture, mixed nitration/halogenation or simple halogenation products were obtained, depending on the conditions used. We were prompted to investigate these reactions because during our initial attempts to nitrate **25** we managed to isolate and characterise a very small amount (*ca*. 2% yield) of the chloro, nitro product **42**. We reasoned that partial decomposition of **25** during the nitration reaction could have released free chloride ions and the presence of these in the nitration mixture could have led to halogenation. We therefore investigated this possibility by deliberately adding halide ion to the nitrating mixture.

When the cationic iridabenzofuran **24** is treated with the standard copper nitrate-acetic anhydride nitrating mixture to which one equivalent of lithium bromide or chloride has been added, halogenation occurs to give **34** or **41** (Scheme 1.14), respectively, as the major products [68]. Substitution occurs at the C6 position, the same position that is brominated when the reaction is carried out with pyridinium tribromide [52]. Minor amounts (<10%) of the mono-nitrated product **38** are also formed in these

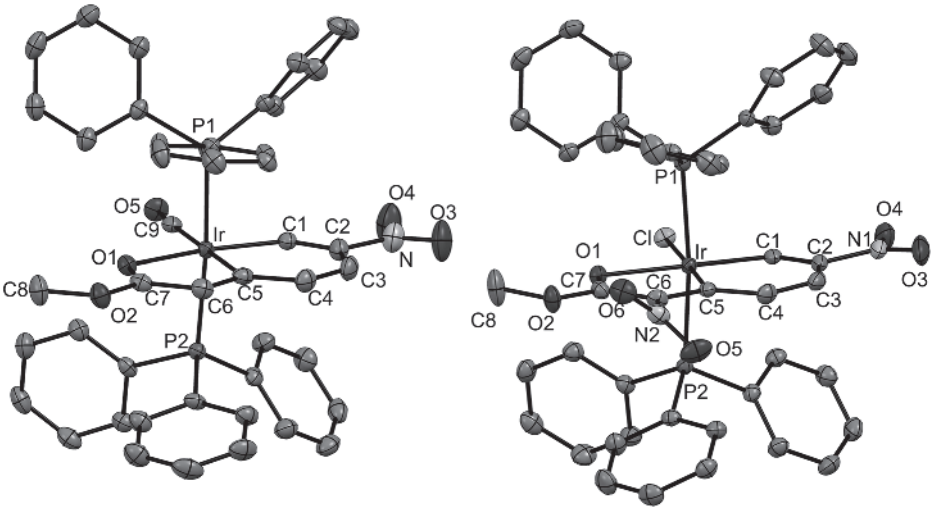

Figure 1.12 Molecular structures of the cation of **38** (left) and **40** (right) showing 50% probability thermal ellipsoids. Hydrogen atoms are not shown for clarity. Selected distances [Å] for **38**: Ir–C1 2.021(4), Ir–C5 2.062(4), Ir–O1 2.186(3), Ir–C9 1.936(4), C1–C2 1.341(6), C2–C3 1.448(6), C3–C4 1.344(6), C4–C5 1.442(5), C5–C6 1.366(6), C6–C7 1.440(6), C7–O1 1.264(5), C2–N 1.488(5). Selected distances [Å] for **40**: Ir–C1 1.963(4), Ir–C5 2.003(4), Ir–O1 2.213(3), Ir–Cl 2.4591(10), C1–C2 1.357(5), C2–C3 1.426(6), C3–C4 1.359(6), C4–C5 1.442(5), C5–C6 1.382(5), C6–C7 1.450(5), C7–O1 1.252(4), C2–N1 1.473(5), C6–N2 1.463(5).

reactions. If two equivalents of lithium bromide are present during nitration of the neutral iridabenzofuran **25**, the dibromoiridabenzofuran **35** is formed (Scheme 1.14) [68]. This is the same product that is obtained by treatment of **24** with pyridinium tribromide [52].

With careful control of the ratio of copper nitrate and lithium chloride, mixed halo, nitro derivatives can be obtained. Thus, if **25** is subjected to nitration with copper nitrate (2.5 equivalents) in the presence of one equivalent of lithium chloride, the C2 site is nitrated while C6 is chlorinated, and the mixed substitution product $Ir(C_7H_3O\{NO_2\text{-}2\}\{Cl\text{-}6\}\{OMe\text{-}7\})Cl(PPh_3)_2$ (**42**) (Scheme 1.14) is obtained as bright red crystals in 47% yield. If a larger amount of copper nitrate (5.0 equivalents) is used in the presence of one equivalent of lithium chloride, trisubstitution occurs with C2 and C4 being nitrated while C6 is chlorinated, to give $Ir(C_7H_2O\{NO_2\text{-}2\}\{NO_2\text{-}4\}\{Cl\text{-}6\}\{OMe\text{-}7\})Cl(PPh_3)_2$ (**43**) in 56% yield as dark red crystals. The former can also be nitrated to give the latter, but in practice the one step process is more convenient and gives better overall yields [68].

The spectroscopic and structural data for the two chloro, nitro-substituted complexes **42** and **43** confirm the formulations and the regioisomers that are formed. In the ^{1}H NMR spectra, H1 is observed at 12.15 ppm in **42** and 12.55 ppm in **43**, down-field shifts which are similar to those found in the other nitroiridabenzofurans. There are only two further aromatic proton resonances observed for **42** (at 5.30 (H4) and 6.39 (H3) ppm), and only one for **43**, (at 7.11 (H3) ppm). In the ^{13}C NMR spectra of **42** and **43**, C6 which bears the chloro-substituent, is found at 110.56 and 112.06 ppm, respectively. Similar up-field shifts were found for the bromine-bearing carbons (*ca*. 110 ppm) in the

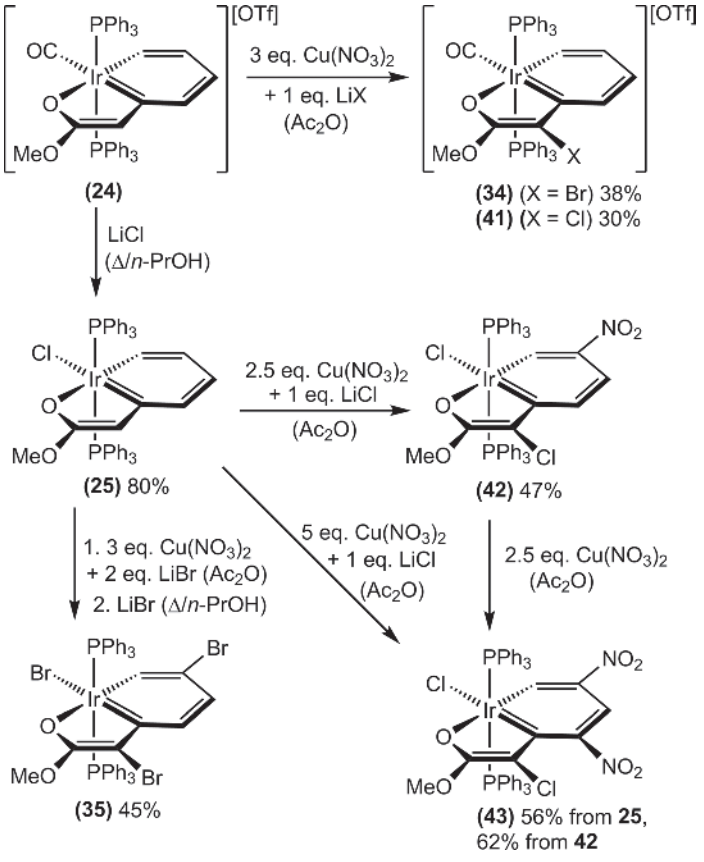

Scheme 1.14 Halogenation and mixed halogenation/nitration products formed by treatment of iridabenzofurans with mixtures of copper nitrate and lithium halides in acetic anhydride.

previously reported iridabenzofurans **34**, **35**, and **37** [52]. As expected, the nitro-bearing carbon atoms resonate in positions similar to the other nitroiridabenzofurans **38–40** (*ca*. 140 ppm), with chemical shifts of 143.36 (C2 in **42**), 143.33 and 143.46 ppm (C2 and C6 in **43**) [68].

Crystal structure determinations of **42** and **43** confirm the substitution patterns in the fused rings. Molecular structures of these compounds are shown in Figure 1.13. Features such as approximately octahedral coordination geometry about iridium, planar fused ring systems and a degree of carbon–carbon bond length alternation are observed in both complexes, just as they are in the other iridabenzofurans. On the basis of the structural and spectroscopic data it does not appear that the π-delocalisation over the fused ring systems is significantly affected by the substituents. In **43** the chloro substituent at C6 and the nitro substituent at C4 are in close proximity and the steric crowding results in the chloro substituent being displaced 0.367 Å above the Ir, C1–C7 O1 least-squares plane and the nitro group rotating out of this plane [68].

Although no direct evidence has been obtained for the mechanism of these reactions that form the mixed halo, nitro iridabenzofuran derivatives, it seems likely that the added chloride reacts with the acetyl nitrate formed in the nitrating mixture [72–74]

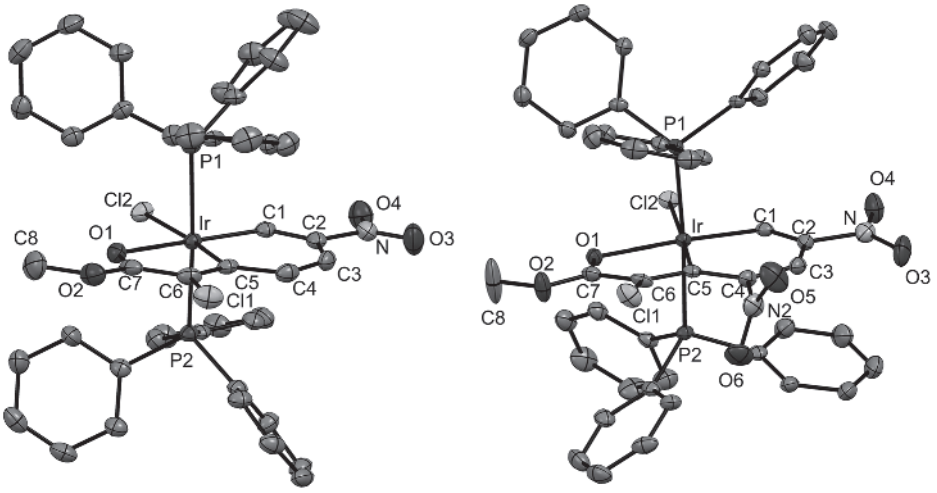

Figure 1.13 Molecular structures of the mixed substitution iridabenzofurans **42** (left) and **43** (right) showing 50% probability thermal ellipsoids. Hydrogen atoms are not shown for clarity. Selected distances [Å] for **42**: Ir–C1 1.965(3), Ir–C5 2.006(3), Ir–O1 2.2122(19), Ir–Cl1 2.4477(9), C1–C2 1.350(4), C2–C3 1.435(4), C3–C4 1.352(4), C4–C5 1.436(4), C5–C6 1.374(4), C6–C7 1.428(4), C7–O1 1.255(4), C2–N 1.475(4), C6–Cl2 1.761(3). Selected distances [Å] for **43**: Ir–C1 1.963(4), Ir–C5 2.017(4), Ir–O1 2.207(3), Ir–Cl1 2.4418(11), C1–C2 1.349(6), C2–C3 1.422(6), C3–C4 1.354(6), C4–C5 1.441(5), C5–C6 1.362(6), C6–C7 1.453(6), C7–O1 1.249(5), C2–N1 1.497(5), C4–N2 1.484(5), C6–Cl2 1.739(4).

to form nitryl chloride and/or chlorine, and one or both of these is the active chlorinating agent [75]. In the case where 2.5 equiv. of $Cu(NO_3)_2$ is used, there is sufficient acetyl nitrate remaining after reaction with the added chloride to introduce only one nitro substituent and ultimately form the observed major product **42** (Scheme 1.14). In the case where 5.0 equiv. of $Cu(NO_3)_2$ is used, there is sufficient acetyl nitrate to effect dinitration in addition to chlorination to give **43** as the major product. Similarly, the dibrominated derivative **35** that is formed on treatment of **25** with $Cu(NO_3)_2$ and LiBr in acetic anhydride (Scheme 1.14) is likely formed through reaction between acetyl nitrate and bromide to form nitryl bromide and/or bromine as the brominating agent [75].

It is worth noting that neither a dichlorinated product nor a mixed bromo/nitro product was detected in the reactions involving copper nitrate, acetic anhydride and lithium halides. However, a mixed bromo/nitro product, $IrCl(C_7H_3O\{NO_2\text{-}2\}\{Br\text{-}6\}\{OMe\text{-}7\})(PPh_3)_2$ (**44**), was obtained on the treatment of **39** with pyridinium tribromide (Scheme 1.15). Bromination of **38**, **40** and **44** did not occur even if up to 5 equiv. of pyridinium tribromide was employed [68].

1.4.2 Rearrangement to Cyclopentadienyl Complexes

One of the important decomposition routes for many metallabenzenes is rearrangement to the corresponding cyclopentadienyl complexes. Clearly, an understanding of the factors that influence this process is important before the rational syntheses of kinetically stable metallabenzenes can be undertaken. Computational studies have

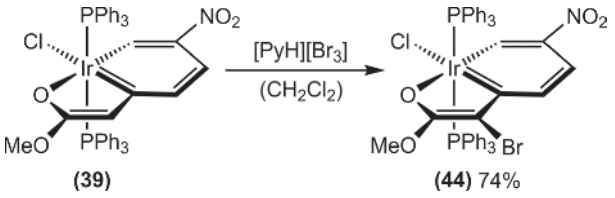

(39) **(44)** 74%

Scheme 1.15 Synthesis of the mixed bromo/nitro iridabenzofuran **44**.

shown that most metallabenzenes are thermodynamically unstable towards this rearrangement and the mechanism of this process has also been studied theoretically [24, 76, 77]. Furthermore, undetected metallabenzenes have been proposed as intermediates in the formation of a number of cyclopentadienyl complexes [42, 62, 78–83]. It is therefore somewhat surprising that well-defined transformations of isolated metallabenzenes into the corresponding cyclopentadienyl complexes have rarely been observed [48, 84–86].

With the isolation of osmabenzene **45** (Scheme 1.16), we had at our disposal the means to synthesise a set of related osmabenzenes that contained different anionic ligands through simple triflate displacement reactions. It was also possible to synthesise a corresponding set of isomeric osmabenzenes via the thermal rearrangement of **3b** in solution (Scheme 1.16). Having these osmabenzenes in hand allowed us to then investigate the influence of different ancillary ligands and the coordination geometry on the relative rates of thermal rearrangement to the corresponding cyclopentadienyl complexes.

The purple osmabenzene $Os(C_5H_4\{SMe\text{-}1\})(\textit{cis}\text{-}O_3SCF_3)(CO)(PPh_3)_2$ (**45**) is formed in high yield through treatment of osmabenzene **1** with methyl triflate (Scheme 1.16). No crystal structure determination of **45** has been obtained, but the products obtained on addition of coordinating anions are consistent with the geometry depicted in Scheme 1.16. On stirring solutions of **45** under ambient conditions with iodide, chloride, thiocyanate or trifluoroacetate the corresponding blue neutral osmabenzenes $Os(C_5H_4\{SMe\text{-}1\})(\textit{cis}\text{-}X)(CO)(PPh_3)_2$ (X = I (**3b**), X = Cl (**46a**), X = SCN (**46b**), X = CF_3CO_2 (**46c**)) are formed (Scheme 1.16). In each case, the anionic ligand is

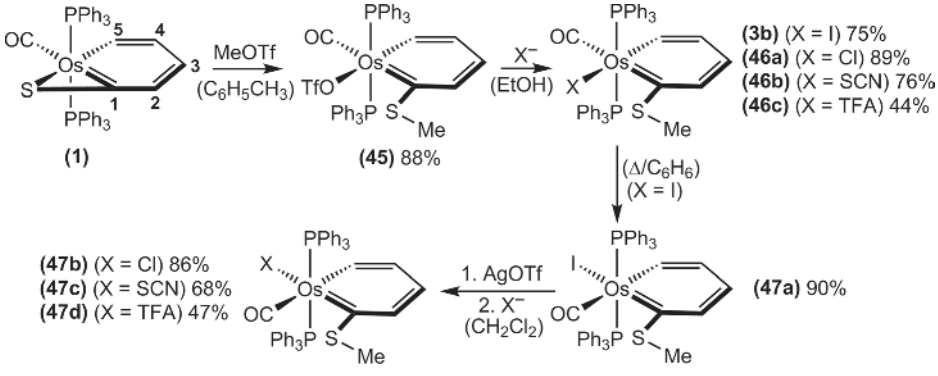

Scheme 1.16 Syntheses of the osmabenzenes **45**, **46a–c** and **47a–d**.

coordinated *cis* to the carbon bearing the methylthiolate group, while the CO ligand is located *trans* to this carbon atom [14, 87, 88].

When the osmabenzene **3b** is heated under reflux in benzene for just 10 min, an isomerisation process occurs in which the positions of the iodide and carbonyl ligands are interchanged, to give the dark-brown osmabenzene, $Os(C_5H_4\{SMe\text{-}1\})$(*trans*-I)$(CO)(PPh_3)_2$ (**47a**), (Scheme 1.16) in 90% yield. In this isomer the iodide ligand is located *trans* to the carbon bearing the –SMe group and the CO ligand *cis* to this carbon atom. None of the other osmabenzenes **46a-c** underwent this particular thermal isomerism on heating in benzene. As expected, small differences are observed in the ^1H and ^{13}C NMR spectra of **3b** and **47a**, the most notable being the shifts in positions of H5 (12.74 and 12.40 ppm for **3b** and **47a**, respectively) and C1 (244.18 and 237.45 ppm for **3b** and **47a**, respectively) [63, 88]. Isolation of **47a** enabled the corresponding series of isomeric osmabenzenes $(Os(C_5H_4\{SMe\text{-}1\})$(*trans*-X)$(CO)(PPh_3)_2$ (X = Cl (**47b**), X = SCN (**47c**), X = CF_3CO_2 (**47d**)) to be synthesised through iodide abstraction by Ag^+ followed by the addition of chloride, thiocyanate or trifluoroacetate, respectively (Scheme 1.16) [88].

With both isomers of each member of this family of osmabenzenes with different anionic ligands available to us, we were then able to study the thermal rearrangement of these compounds to the corresponding cyclopentadienyl complexes. It was convenient to study these rearrangements in refluxing toluene solutions because many of the rearrangements occurred at reasonable rates under these conditions. It was found that two osmium cyclopentadienyl products were formed, and these were the cationic bis(triphenylphosphine) cyclopentadienyl complexes **48a–e** and the neutral mono(triphenylphosphine) cyclopentadienyl complexes **49a–c** (Scheme 1.17). The identities and yields of each of the cyclopentadienyl compounds formed were monitored by NMR spectroscopy and mass spectrometry. In most cases the two cyclopentadienyl complexes could be isolated as pure compounds [88].

It was found that the ratio of the two cyclopentadienyl products obtained and the rate at which they formed under these conditions were highly dependent on the nature of the anionic ligand and the relative geometry of this and the adjacent CO ligand with respect to the SMe-substituted osmabenzene ring.

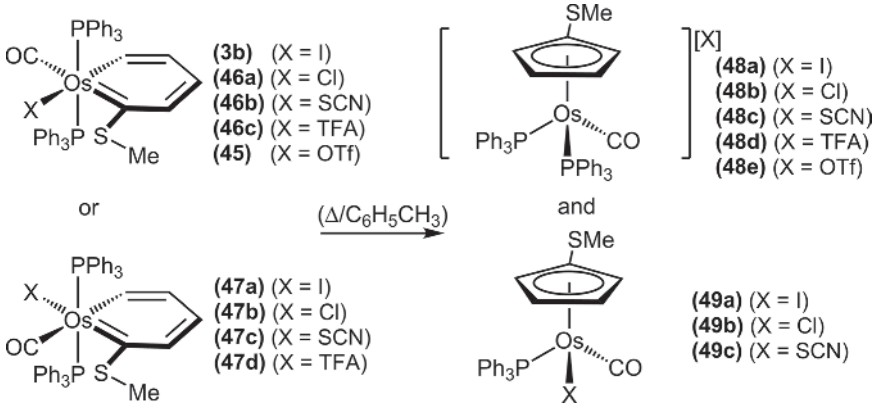

Scheme 1.17 Thermal rearrangement reactions of the osmabenzenes **3b**, **45**, **46a–c** into the osmium cyclopentadienyl complexes **48a–e** and **49a–c**.

With regard to the blue osmabenzenes **3b**, **45** and **46a–c**, in each case mixtures of the two cyclopentadienyl complexes were obtained. Osmabenzene **3b** gave **48a** and **49a** in a 40:60 ratio, **46a** gave **48b** and **49b** in a 75:25 ratio and **46b** gave **48c** and **49c** in a 50:50 ratio. In each of these three cases, approximately 1 h of heating under reflux was required to fully convert the osmabenzene to the cyclopentadienyl products. In contrast, the analogous trifluoroacetate derivative **46c** gave the cationic cyclopentadienyl complex **48d** as the exclusive product within minutes. The trifluoromethane sulfonate derivative **45** is not soluble in toluene and so thermal rearrangement of this osmabenzene was studied in the lower boiling point solvent 1, 2-dichloroethane. As for **46c**, exclusive rearrangement to the corresponding cationic cyclopentadienyl complex **48e** occurred within minutes.

The brown osmabenzenes **47a** and **47b** showed very similar behaviour to the isomeric compounds **3b** and **46a**, in that mixtures of the two cyclopentadienyl complexes were formed over 1 h and in exactly the same ratios as were obtained from the thermal rearrangements of **3b** and **46a**. It is very likely that the first step in the thermal rearrangements of **3b** and **46a** is isomerisation into **47a** and **47b**. In contrast, the brown osmabenzenes **47c** (SCN *trans* to CSMe) and **47d** (CF_3CO_2 *trans* to CSMe) completely resisted rearrangement into cyclopentadienyl products and were recovered essentially unchanged after heating under reflux in toluene for 1 h. This is in stark contrast to the corresponding isomers (**46b** and **46c**, respectively), both of which readily underwent conversion to cyclopentadienyl products [88].

The molecular structures of two representative examples of the cyclopentadienyl products, **48b** and **49a**, is shown in Figure 1.14.

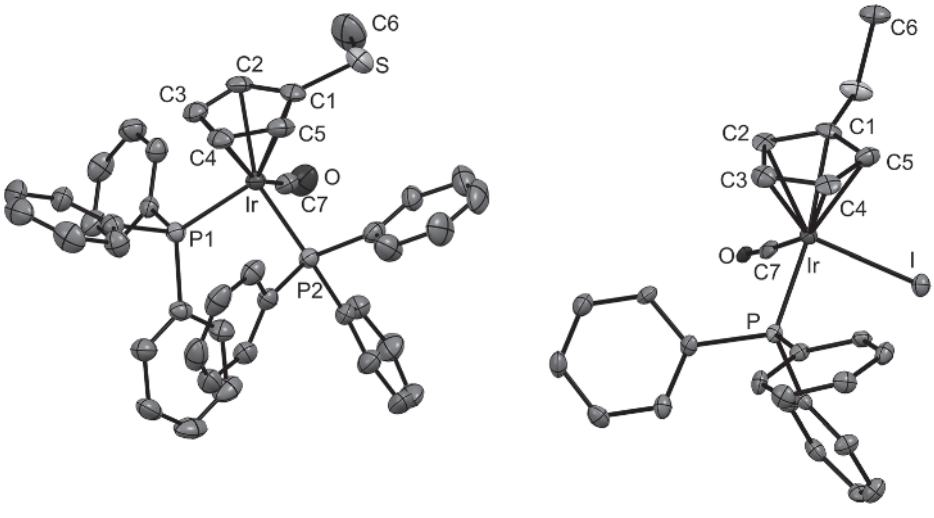

Figure 1.14 Molecular structures of the cation of **48d** (left) and **49a** (right) showing 50% probability thermal ellipsoids. Hydrogen atoms are not shown for clarity. Selected distances [Å] for **48d**: Os–C1 2.327(5), Os–C2 2.275(5), Os–C3 2.243(5), Os–C4 2.266(5), Os–C5 2.292(5), Os–C7 1.857(6), Os–P1 2.3539(14), Os–P2 2.3661(14), C1–C2 1.452(8), C2–C3 1.415(8), C3–C4 1.438(8), C4–C5 1.420(9), C5–C1 1.439(8). Selected distances [Å] for **49a**: Os–C1 2.255(7), Os–C2 2.222(7), Os–C3 2.215(8), Os–C4 2.305(7), Os–C5 2.298(10), Os–C7 1.880(11), Os–P 2.2963(18), Os–I 2.7253(5), C1–C2 1.436(11), C2–C3 1.412(12), C3–C4 1.418(12), C4–C5 1.428(14), C5–C1 1.407(11).

These results show that the rates of thermal rearrangements of metallabenzenes to cyclopentadienyl complexes can be highly sensitive to the nature of the anionic ancillary ligands and to the coordination geometry about the metal. While no direct evidence was obtained for the mechanisms of these rearrangements to cyclopentadienyl products, two important observations were made. First, the cationic and neutral cyclopentadienyl products **48a** and **49a** do not interconvert under the same or similar reaction conditions to those used in the formation of these compounds. These observations strongly suggest that the cyclopentadienyl products **48a–e** and **49a–c** are formed independently via two different pathways. Second, if the osmabenzene **47a** is heated under reflux in toluene in the presence of 10 equivalents of triphenylphosphine, the ratio of the two cyclopentadienyl products formed changes markedly in favour of cationic bis(triphenylphosphine) product **48a** (90%) over neutral mono(triphenylphosphine) product **49a** (10%). This suggests that PPh_3 dissociation is involved in the rate-determining step of the pathway to **49a**. Further, more detailed studies are needed to learn more about the mechanisms of these reactions [88].

It is noted in Section 1.3.2 above that the ruthenabenzofuran $Ru(C_7H_3O\{CO_2Me\text{-}2\}\{CO_2Me\text{-}4\}\{OMe\text{-}7\})(CO)(PPh_3)_2$ (**19**) is remarkably thermally robust. Furthermore, treatment of a refluxing benzene/methanol solution of **19** with trimethylsilyl chloride (an anhydrous HCl source) while simultaneously irradiating with visible light over a period of 4–5 h gives the green, tethered ruthenabenzene, $Ru(C_5H_2\{CO_2Me\text{-}2\}\{CO_2Me\text{-}4\}\{CH_2C(O)OMe\text{-}5\})Cl(PPh_3)_2$ (**21**), in very good yield (78%). The other product that can be isolated in *ca.* 10% yield from this reaction is the ruthenium cyclopentadienyl complex $Ru(\eta^5\text{-}C_5H_2\{CO_2Me\text{-}2\}\{CO_2Me\text{-}4\}\{CH_2CO_2Me\text{-}5\}Cl(CO)(PPh_3)$ (**50**) (Scheme 1.18). This product presumably forms through rearrangement of the tethered ruthenabenzene **21** under the vigorous reaction conditions. It is remarkable that **21** does not decompose at a faster rate under these conditions. The tethering arm and the electron-withdrawing ester functions probably make significant contributions to the stability of **21** [42].

1.4.3 Nucleophilic Aromatic Substitution Reactions

The previous two sections illustrate the important general observation that some reactions which metallabenzenes undergo mirror those classically associated with benzene itself (e.g. electrophilic aromatic substitution), while others have no counterpart in benzene chemistry (e.g. rearrangement to cyclopentadienyl ligands) [22, 34, 59, 60, 89–92].

Nucleophilic aromatic substitution (S_NAr) is a reaction class that is classically associated with benzene and its derivatives. Traditionally, S_NAr proceeds by the addition of a nucleophile to a carbon atom of a suitably electron-deficient (and hence activated

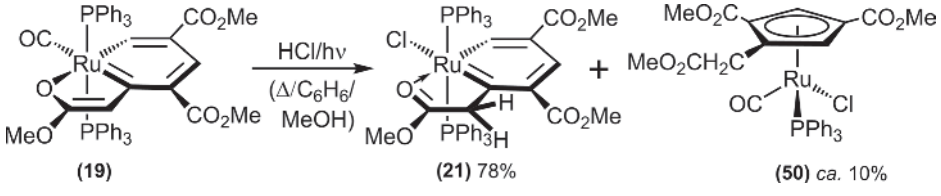

Scheme 1.18 Rearrangement of the ruthenabenzofuran **19** into the cyclopentadienyl complex **50**, as a side product during the synthesis of the tethered ruthenabenzene **21**.

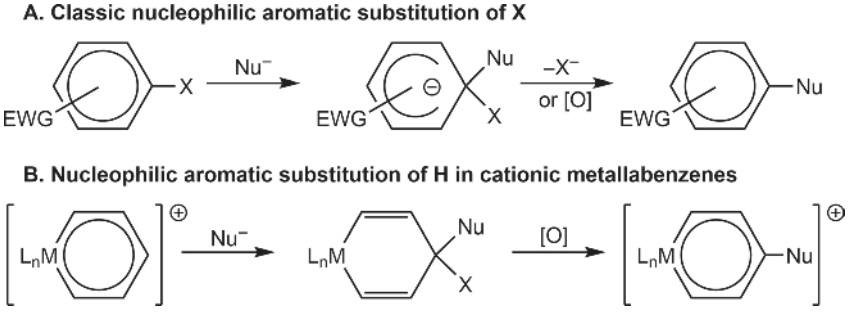

Chart 1.5 Nucleophilic aromatic substitution (S_NAr) of leaving group X (A) or H (B) in benzenes with electron withdrawing groups (EWGs), and the S_NAr of H in cationic metallabenzenes.

benzene) ring. This forms an intermediate σ^X-adduct. If this site of attack is occupied by a good leaving group X, then the substituted benzene product is obtained through loss of X^- (Chart 1.5A). If instead it is occupied by hydrogen (X = H), the elimination of hydride from the σ^H-adduct is much less favourable and an additional process is often required to convert it into the substituted product. This is usually achieved by oxidation of the σ^H-adduct, or by the elimination of HY from it (where Y is a secondary group that is present as part of the nucleophile or as a substituent on the aromatic ring).

During our studies of the chemistry of iridabenzenes and osmabenzenes, we had synthesised a small number of cationic derivatives which had tightly coordinating and chemically robust ancillary ligands. It occurred to us that if these compounds were treated with nucleophiles, attack might be directed towards one of the metallabenzene ring carbon atoms rather than to the metal. If this did happen then the product formed would be very closely related to the σ^X-adducts formed as intermediates in S_NAr reactions of benzenes (Chart 1.5). Oxidation of any metallacyclohexadiene intermediate thus formed could then yield the corresponding substituted metallabenzene.

Two metallabenzenes that seemed to be good candidates for investigating reactions of this type were the red osmabenzene $[Os(C_5H_4\{SMe\text{-}1\})(CO)_2(PPh_3)_2][OTf]$ (**51**) (which can be prepared by treating **1** with methyl triflate and then CO) and the green iridabenzene $[Ir(C_5H_4\{SMe\text{-}1\})(\kappa^2\text{-}S_2CNEt_2)(PPh_3)_2][PF_6]$ (**52**) (which can be simply obtained as the PF_6^- salt from the iridabenzene **13** by replacing the two labile chloride ligands with a bidentate diethyldithiocarbamate ligand) (Scheme 1.19) [64]. Both metallabenzenes are cationic which we reasoned may reduce the electron density in the metallacyclic rings and facilitate attack by negatively charged nucleophiles. In addition, in both complexes there is only one ring substituent, and so steric hindrance to attack by nucleophiles should be minimal.

Indeed, we found that on treatment of either **51** or **52** with sodium borohydride in ethanol the bright colours of the metallabenzenes fade and the colourless neutral metallacyclohexa-1,4-diene complexes $Os(C_5H_3\{SMe\text{-}1\}\{H_2\text{-}3\})(CO)_2(PPh_3)_2$ (**53a**) or $Ir(C_5H_3\{SMe\text{-}1\}\{H_2\text{-}3\})(\kappa^2\text{-}S_2CNEt_2)(PPh_3)_2$ (**54a**), respectively, precipitate from solution (Scheme 1.19). In each case hydride adds to the C3 carbon of the metallabenzene ring, saturating this carbon atom and disrupting the π-electron delocalisation about the metallacyclic ring. These reactions are highly regioselective with the only products detected resulting from nucleophilic addition at C3 [64]. In a related reaction, it had

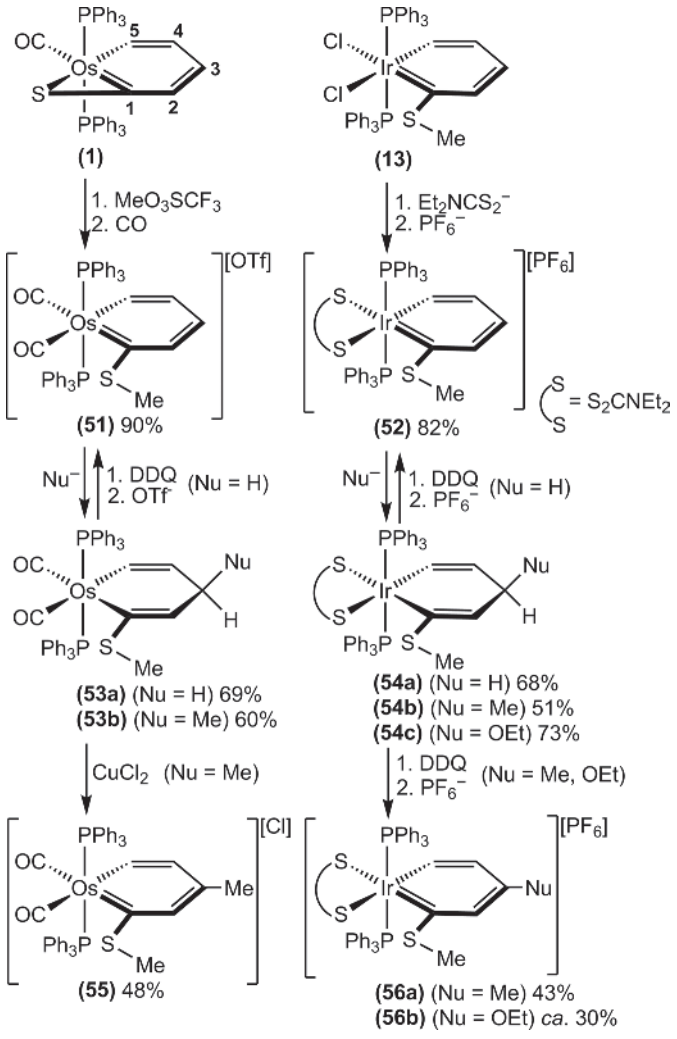

Scheme 1.19 Nucleophilic aromatic substitution reactions of osmabenzenes and iridabenzenes.

previously been reported that hydroxide ion adds reversibly to the same position of a very different iridabenzene, also forming an iridacyclohexadiene [56, 93]. Details of this reaction are provided in Chapter 4.

Loss of the delocalised π-system of the metallabenzene rings of **51** and **52** causes substantial changes to the spectroscopic and structural properties of the resulting complexes. For example, in the ^{1}H NMR spectrum of the osmabenzene **51**, H5 appears at the down-field position of 10.82 ppm while the signal for this same proton moves up-field to 7.08 ppm in the corresponding osmacyclohexa-1,4-diene, **53a**. As expected, the signal for H3 moves considerably up-field (from 7.08 ppm to 2.01 ppm) as C3 becomes saturated in **53a**. The resonances of the ring carbon atoms in the ^{13}C NMR spectra of **51** and **53a** are also significantly different. Loss of the delocalised π-system in **51** causes up-field shifts of close to 100 ppm in the metal-bound carbon atoms

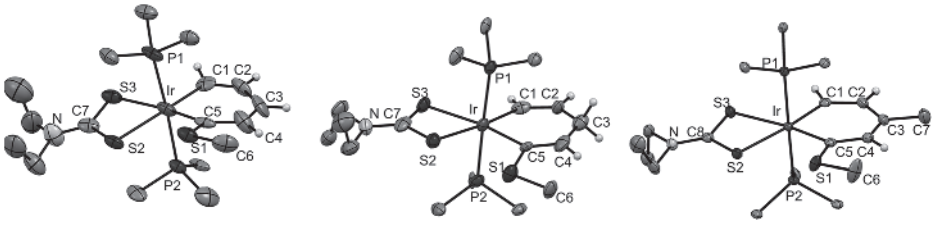

Figure 1.15 Molecular structures of the cation of **52** (left), **54a** (centre) and **56a** (right) showing 50% probability thermal ellipsoids. Phenyl rings on the triphenylphosphine ligands and most hydrogen atoms are not shown for clarity. Selected distances [Å] for **52**: Ir–C1 2.009(16), Ir–C5, 2.009(16), C1–C2, 1.42(2), C2–C3, 1.36(2), C3–C4, 1.44(2), C4–C5, 1.31(2). Selected distances [Å] for **54a**: Ir–C1 2.046(11), Ir–C5 2.073(12), C1–C2 1.321(16), C2–C3 1.460(18), C3–C4 1.465(16), C4–C5 1.340(16). Selected distances [Å] for **56a**: Ir–C1 2.011(3), Ir–C5 2.014(3), C1–C2 1.389(5), C2–C3 1.382(5), C3–C4 1.425(5), C4–C5 1.363(4), C3–C7 1.503(5). (*See color plate section for the color representation of this figure.*)

(from 250.97 (C1) and 199.58 (C5) ppm in **51** to 132.88 (C1) and 123.35 (C5) ppm in **53a**). C3 also shifts from an aromatic position in **51** (154.32 ppm) to a saturated position in **53a** (38.85 ppm). Very similar changes in the chemical shifts of the metallacyclic ring atoms are observed in the NMR spectra of the iridabenzene **52** when it is converted into the iridacyclohexa-1,4-diene **54a** [64].

Crystal structures of the cationic iridabenzene **52** and the corresponding iridacyclohexa-1,4-diene derivative **53a** have been obtained (Figure 1.15). From the structure of **52** it can be seen that the Ir–C and C–C distances within the six-membered metallacyclic ring (Ir–C1 2.009(16), Ir–C5 2.009(16), C1–C2 1.42(2), C2–C3 1.36(2), C3–C4 1.44(2), C4–C5 1.31(2) Å) are consistent with a metallabenzene formulation. In comparison, the corresponding distances within the six-membered metallacyclic ring of **54a** are consistent with a metallacyclohexa-1,4-diene formulation. Thus, the longer iridium–carbon bonds are close to single bond distances (Ir–C1 2.046(11), Ir–C5 2.073(12) Å), the C1–C2 and C4–C5 bond lengths (1.321(16) and 1.340(16) Å, respectively) are consistent with double bonds, and the C2–C3 and C3–C4 distances (1.460(18) and 1.465(16) Å, respectively) are appropriate for single bonds [64].

Other nucleophiles also add to the ring C3 atoms of **51** and **52** to form related metallacyclohexadiene complexes. For example, treatment of **51** or **52** with methyllithium yields the colourless $Os(C_5H_3\{SMe\text{-}1\}\{H\text{-}3\}\{Me\text{-}3\})(CO)_2(PPh_3)_2$ (**53b**) or $Ir(C_5H_3\{SMe\text{-}1\}\{H\text{-}3\}\{Me\text{-}3\})(\kappa^2\text{-}S_2CNEt_2)(PPh_3)_2$ (**54b**), respectively (Scheme 1.19). The iridabenzene cation **52** will also react with sodium ethoxide in ethanol to yield $Ir(C_5H_3\{SMe\text{-}1\}\{H\text{-}3\}\{OEt\text{-}3\})(\kappa^2\text{-}S_2CNEt_2)(PPh_3)_2$ (**53c**). The signals for the metallacyclohexadiene ring atoms in the ^1H and ^{13}C NMR spectra of these complexes are very similar to those observed for **53a** and **54a**. However, in the ^{31}P NMR spectra, significant differences are observed. Unlike the singlet signals that are observed for the two equivalent phosphorus atoms in each of the complexes **53a** and **54a**, four-line second-order spectra are observed for the phosphorus atoms of **53b**, **54b** and **53c**. In these complexes the addition of the methyl or ethoxide groups to C3 removes the horizontal mirror plane that was present in the substrate metallabenzenes, and the two phosphorus atoms become inequivalent. The chemical shift difference between the two phosphorus atoms in each case is of the same order as the coupling constant, which gives rise to the second-order spectra [64].

These highly regioselective nucleophilic additions can also be rationalised by consideration of the condensed Fukui functions for the ring carbon atoms. The computed f_k^+ values for the osmabenzene **51** and iridabenzene **52** indicate that C3 is the most electrophilic atom, followed closely by C5 and C1. Nucleophilic attack should therefore be electronically favourable at each of these three sites. The observed exclusive preference for attack at C3 is most likely due to the C1 and C5 sites being sterically shielded by the metal and its ancillary ligands [64].

These metallacyclohexa-1,4-dienes can be considered intermediates akin to the σ^H-adducts formed during S_NAr reactions of benzenes. The possibility of oxidising these compounds to give the corresponding substituted metallabenzenes was therefore investigated. It was found that treatment with a range of oxidants including 2,3-dichloro-5,6-dicyano-1,4-benzoquinone (DDQ), copper(II) chloride or oxygen results in rearomatisation of the metallacyclohexa-1,4-diene rings and formation of the corresponding metallabenzenes. In the case of **53a** or **54a**, where hydride had been added to C3 of the cationic metallabenzenes **51** or **52**, respectively, treatment with each of these oxidants returned the starting metallabenzenes after addition of a salt containing the appropriate counteranion (Scheme 1.19). In these reactions the highest yields were obtained with DDQ. Oxidation of the methyl-substituted osmacyclohexadiene **53b** gave the methyl-substituted osmabenzene $[Os(C_5H_3\{SMe\text{-}1\}\{Me\text{-}3\})(CO)_2(PPh_3)_2][Cl]$ (**55**) as purple crystals. In this case the best yields were obtained if $CuCl_2$ was used as the oxidant (Scheme 1.19). In a similar manner, oxidation of the iridacyclohexadienes **54b** or **54c** gave the methyl-substituted iridabenzene $[Ir(C_5H_3\{SMe\text{-}1\}\{Me\text{-}3\})(\kappa^2\text{-}S_2CNEt_2)(PPh_3)_2][PF_6]$ (**56a**) or the ethoxy-substituted iridabenzene $[Ir(C_5H_3\{SMe\text{-}1\}\{OEt\text{-}3\})(\kappa^2\text{-}S_2CNEt_2)(PPh_3)_2][PF_6]$ (**56b**), respectively. DDQ was found to be the oxidant that gave the highest yields of the products in these cases [64].

The spectroscopic and structural data obtained for the substituted metallabenzene products closely resemble those found for the starting metallabenzenes **51** and **52**. For osmabenzene **55** the ring methyl substituent is observed as a singlet at 1.74 ppm in the ^{1}H NMR spectrum. The remaining osmabenzene ring signals observed in the ^{1}H NMR (5.89 (H2), 6.97 (H4), 10.86 (H5) ppm) and ^{13}C NMR (245.91 (C1), 126.15 (C2), 171.28 (C3), 139.89 (C4), 197.04 (C5) ppm) spectra are almost identical to those of the precursor osmabenzene **51**. Re-establishment of the osmabenzene ring also restores the equatorial mirror plane, and once more only one singlet is observed in the ^{31}P NMR spectrum for the two equivalent phosphorus atoms [64].

Re-establishment of the iridabenzene ring is also evident in the NMR spectra of the methyl-substituted iridabenzene **56a** as well as in the ethoxy-substituted iridabenzene **56b**. In each case the ^{1}H and ^{13}C NMR spectra of the ring atoms resemble those of the corresponding parent iridabenzene **52**. The bond lengths about the metallacyclic rings in the crystal structures of **56a** (Figure 1.15) (Ir–C1 2.011(3), Ir–C5 2.014(3), C1–C2 1.389(5), C2–C3 1.382(5), C3–C4 1.425(5), C4–C5 1.363(4) Å) and **56b** (Ir–C1 2.022(16), Ir–C5 1.996(13), C1–C2 1.35(2), C2–C3 1.40(2), C3–C4 1.447(19), C4–C5, 1.349(19) Å) also support re-establishment of the delocalised π-systems. In each case the Ir–C and C–C bond distances are appropriate for iridabenzene formulations [64]. Related reactions of metallabenzenes involving intramolecular nucleophilic substitution [51, 94] and *cine*-substitution [95] have also been reported, and these are discussed in Chapter 6.

The sequence of reactions that take the cationic metallabenzenes **51** and **52** to the corresponding metallacyclohexadienes and then to the corresponding substituted

cationic metallabenzenes mimics the steps involved in the classic nucleophilic aromatic substitution of hydrogen (S_NAr^H) in benzene chemistry. These reactions therefore provide a further example of where the chemistry of metallabenzenes and benzene overlap.

1.5 Concluding Remarks

Our involvement in both the inception and the subsequent development of the field of metallabenzene chemistry has been a very rewarding experience. From the outset we have been privileged to have worked with some outstanding and highly talented students and it is largely through their hard work and dedication that we have been able to make our particular contributions to this area. In our studies we have been able to develop efficient synthetic routes to metallabenzenes that bear only one ring substituent, synthesise and study a number of interesting fused-ring and tethered metallabenzenes, discover examples of metallabenzene reactions involving electrophilic aromatic substitution and nucleophilic aromatic substitution of hydrogen, as well as study well-defined rearrangements of metallabenzenes to cyclopentadienyl compounds. Many exciting challenges remain in the field of metallabenzene chemistry and we are confident that the field will continue to flourish and capture the imagination of chemists for many years to come.

References

1 Faraday, M. (1825) On new compounds of carbon and hydrogen, and on certain other products obtained during the decomposition of oil by heat. *Philosophical Transactions of the Royal Society of London*, **115**, 440–466.
2 Mitscherlich, E. (1834) Ueber das Benzol und die Säuren der Oel- und Talgarten. *Annalen der Pharmacie*, **9**(1), 39–48.
3 Kekulé, A. (1865) Sur la constitution des substances aromatiques. *Bulletin de la Societe Chimique de France*, **3**, 98–110.
4 Kekulé, F. A. (1865) Note sur quelques produits de substitution de la benzine. *Bulletin De l'Academie Royale De Medecine De Belgique*, **19**, 551–563.
5 Anderson, T. (1851) Ueber die Producte der trocknen Destillation thierischer Materien. *Justus Liebigs Annalen der Chemie*, **80**(1), 44–65.
6 Märkl, G., Lieb, F., Merz , A. (1967) A new synthesis of phosphabenzene derivatives. *Angewandte Chemie: International Edition*, **6**(5), 458–459.
7 Ashe, A. J. (1971) Phosphabenzene and arsabenzene. *Journal of the American Chemical Society*, **93**(13), 3293–3295.
8 Ashe, A. J. and Chan, W.-T. (1979) Preparation of 2-substituted arsabenzenes. *Journal of Organic Chemistry*, **44**(9), 1409–1413.
9 Wakita , K., Tokitoh, N., Okazaki, R. and Nagase, S. (2000) Synthesis and properties of an overcrowded silabenzene stable at ambient temperature. *Angewandte Chemie: International Edition*, **39**(3), 634–636.
10 Ashe, A. J., Diephouse, T. R. and El-Sheikh, M. Y. (1982) Stabilization of stibabenzene and bismabenzene by 4-alkyl substituents. *Journal of the American Chemical Society*, **104**(21), 5693–5699.

11 Nakata, N., Takeda, N. and Tokitoh, N. (2002) Synthesis and properties of the first stable germabenzene. *Journal of the American Chemical Society*, **124**(24), 6914–6920.

12 Mizuhata, Y., Noda, N. and Tokitoh, N. (2010) Generation of stannabenzenes and their properties. *Organometallics*, **29**(21), 4781–4784.

13 Thorn, D. L. and Hoffmann, R. (1979) Delocalization in metallocycles. *Nouveau Journal De Chimie*, **3**(1), 39–45.

14 Elliott, G. P., Roper, W. R. and Waters, J. M. (1982) Metallacyclohexatrienes or "metallabenzenes": Synthesis of osmabenzene derivatives and X-ray crystal structure of [Os(CSCHCHCHCH)(CO)(PPh_3)$_2$]. *Journal of the Chemical Society: Chemical Communications*, **14**, 811–813.

15 Fraser, P. J., Roper, W. R. and Stone, F. G. A. (1974) Carbene complexes of iridium, rhodium, manganese, chromium, and iron containing thiazolidinylidene and pyridinylidene ligands. *Journal of the Chemical Society: Dalton Transactions*, **7**, 760–764.

16 Clark, G. R., Roper, W. R. and Wright, A. H. (1982) Synthesis, structure, and reactions of $IrCl_3(CCl_2)(PPh_3)_2$: A compound with an iridium–carbon double bond ($L_nIr{=}CCl_2$). *Journal of Organometallic Chemistry*, **236**(1), C7–C10.

17 Clark, G. R., Marsden, K., Roper, W. R. and Wright, L. J. (1980) An osmium-carbyne complex. *Journal of the American Chemical Society*, **102**(21), 6570–6571.

18 Clark, G. R., Cochrane, C. M., Roper, W. R. and Wright, L. J. (1980) The interaction of an osmium–carbon triple bond with copper(I), silver(I) and gold(I) to give mixed dimetallocyclopropene species and the structures of Os(AgCl)(CR)Cl(CO)(PPh_3)$_2$. *Journal of Organometallic Chemistry*, **199**(2), C35–C38.

19 Collins, T. J. and Roper, W. R. (1977) Hydrido-thiocarbonyl complexes as precursors of low-valent thiocarbonyl complexes. *Journal of Organometallic Chemistry*, **139**(2), C56–C58.

20 Collins, T. J., Roper, W. R. and Town, K. G. (1976) Synthesis of low-valent thiocarbonyl complexes via 1, 2-elimination of methylthiol from cis-metal-hydrido-dithiomethylester complexes: Os(CS)(CO)$_2$(PPh_3)$_2$ and IrCl(CS)(PPh_3)$_2$. *Journal of Organometallic Chemistry*, **121**(2), C41–C44.

21 Clark, G. R., Marsden, K., Roper, W. R. and Wright, L. J. (1980) Carbonyl, thiocarbonyl, selenocarbonyl, and tellurocarbonyl complexes derived from a dichlorocarbene complex of osmium. *Journal of the American Chemical Society*, **102**(3), 1206–1207.

22 Frogley, B. J. and Wright, L. J. (2014) Fused-ring metallabenzenes. *Coordination Chemistry Reviews*, **270–271**, 151–166.

23 Elliott, G. P., McAuley, N. M., Roper, W. R. and Shapley, P. A. (1989) An osmium containing benzene analog, Os(CSCHCHCHCH)(CO)(PPh_3)$_2$, carbonyl(5-thioxo-1,3-pentadiene-1,5-diyl-C^1,C^5,S)bis(triphenylphosphine)osmium, and its precursors. In: *Inorganic Syntheses*, New York: John Wiley & Sons, Inc., 184–189.

24 Iron, M. A., Lucassen, A. C. B., Cohen, H., *et al.* (2004) A computational foray into the formation and reactivity of metallabenzenes. *Journal of the American Chemical Society*, **126**(37), 11699–11710.

25 Rickard, C. E. F., Roper, W. R., Woodgate, S. D. and Wright, L. J. (2001) Reaction between the thiocarbonyl complex, Os(CS)(CO)(PPh_3)$_3$, and propyne: Crystal structure of a new sulfur-substituted osmabenzene. *Journal of Organometallic Chemistry*, **623**(1–2), 109–115.

26 Orpen, A. G., Brammer, L., Allen, F. H., *et al.* (1989) Supplement: Tables of bond lengths determined by X-ray and neutron diffraction: Part 2: Organometallic

compounds and co-ordination complexes of the d-and f-block metals. *Journal of the Chemical Society: Dalton Transactions*, **12**, S1–S83.

27 Wright, L. J. (2006) Metallabenzenes and metallabenzenoids. *Dalton Transactions*, **15**, 1821–1827.

28 Chin, C. S., Park, Y., Kim, J. and Lee, B. (1995) Facile insertion of alkynes into Ir–P (phosphine) and Ir–As (arsine) bonds: Second and third alkyne addition to mononuclear iridium complexes. *Journal of the Chemical Society: Chemical Communications*, **15**, 1495–1496.

29 Vaska, L. and DiLuzio, J. W. (1961) Carbonyl and hydrido-carbonyl complexes of iridium by reactions with alchols: Hydrido complexes by reaction with acid. *Journal of the American Chemical Society*, **83**(12), 2784–2785.

30 Reed, C. A. and Roper, W. R. (1973) The iridium(I) cation, $[Ir(CO)(CH_3CN)(PPh_3)_2]^+$ and its substitution reactions. *Journal of the Chemical Society: Dalton Transactions*, **13**, 1365–1370.

31 Lu, G.-L., Roper, W. R., Wright, L. J. and Clark, G. R. (2005) A 2-iridathiophene from reaction between $IrCl(CS)(PPh_3)_2$ and $Hg(CHCHPh)_2$. *Journal of Organometallic Chemistry*, **690**(4), 972–981.

32 Dalebrook, A. F. and Wright, L. J. (2009) Annulation of an iridabenzene through formal cycloaddition reactions with organonitriles. *Organometallics*, **28**(18), 5536–5540.

33 Clark, G. R., Johns, P. M., Roper, W. R. and Wright, L. J. (2008) A stable iridabenzene formed from an iridacyclopentadiene where the additional ring-carbon atom is derived from a thiocarbonyl ligand. *Organometallics*, **27**(3), 451–454.

34 Dalebrook, A. F. and Wright, L. J. (2012) Chapter Three: Metallabenzenes and metallabenzenoids. In: *Advances in Organometallic Chemistry*, F. H. Anthony, J. F. Mark (eds), London: Academic Press, Elsevier, **60**, 93–177.

35 Zhu, J., Jia, G. and Lin, Z. (2007) Understanding nonplanarity in metallabenzene complexes. *Organometallics*, **26**(8), 1986–1995.

36 Elliott, G. P. and Roper, W. R. (1983) Metallacyclobutadiene complexes from ligand combination of cs and acetylene on osmium. *Journal of Organometallic Chemistry*, **250**(1), C5–C8.

37 Burrell, A. K., Elliott, G. P., Rickard, C. E. F. and Roper, W. R. (1990) The X-ray structure of $Os(CS)(PhCCPh)(PPh_3)_2$: A complex containing a four-electron donor acetylene ligand. *Applied Organometallic Chemistry*, **4**(5), 535–542.

38 Clark, G. R., Johns, P. M., Roper, W. R. and Wright, L. J. (2006) An osmabenzofuran from reaction between $Os(PhC{\equiv}CPh)(CS)(PPh_3)_2$ and methyl propiolate and the C-protonation of this compound to form a tethered osmabenzene. *Organometallics*, **25**(7), 1771–1777.

39 Chin, C. S., Won, G., Chong, D., *et al.* (2002) Carbon–carbon bond formation involving reactions of alkynes with group 9 metals (Ir, Rh, Co): Preparation of conjugated olefins. *Accounts of Chemical Research*, **35**(4), 218–225.

40 Chin, C. S. and Lee, H. (2004) New iridacyclohexadienes and iridabenzenes by [2+2+1] cyclotrimerization of alkynes and facile interconversion between iridacyclohexadienes and iridabenzenes. *Chemistry: A European Journal*, **10**(18), 4518–4522.

41 Chin, C. S., Lee, H. and Eum, M.-S. (2005) Iridabenzenes from iridacyclopentadienes: Unusual C–C bond formation between unsaturated hydrocarbyl ligands. *Organometallics*, **24**(20), 4849–4852.

42 Clark, G. R., O'Neale, T. R., Roper, W. R., *et al.* (2009) Stable cationic and neutral ruthenabenzenes. *Organometallics*, **28**(2), 567–572.

43 Xia, H., He, G., Zhang, H., *et al.* (2004) Osmabenzenes from the reactions of HC≡CCH(OH)C≡CH with $OsX_2(PPh_3)_3$ (X = Cl, Br). *Journal of the American Chemical Society*, **126**(22), 6862–6863.

44 Gong, L., Chen, Z., Lin, Y., *et al.* (2009) Osmabenzenes from osmacycles containing an η^2-coordinated olefin. *Chemistry: A European Journal*, **15**(25), 6258–6266.

45 Zhang, H., Wu, L., Lin, R., *et al.* (2009) Synthesis, characterization and electrochemical properties of stable osmabenzenes containing PPh_3 substituents. *Chemistry: A European Journal*, **15**(14), 3546–3559.

46 Yamazaki, H. and Aoki, K. (1976) A novel six-membered ruthenium metallocycle. *Journal of Organometallic Chemistry*, **122**(3), C54–C58.

47 Bruce, M. I., Hall, B. C., Skelton, B. W., *et al.* (2000) Some Pentamethylcyclopentadienyl-ruthenium derivatives of methyl propiolate. *Australian Journal of Chemistry*, **53**(2), 99–107.

48 Yang, J., Jones, W. M., Dixon, J. K. and Allison, N. T. (1995) Detection of a ruthenabenzene, ruthenaphenoxide, and ruthenaphenanthrene oxide: The first metalla aromatics of a second-row transition metal. *Journal of the American Chemical Society*, **117**(38), 9776–9777.

49 Zhang, H., Xia, H., He, G., *et al.* (2006) Synthesis and characterization of stable ruthenabenzenes. *Angewandte Chemie: International Edition*, **45**(18), 2920–2923.

50 Zhang, H., Feng, L., Gong, L., *et al.* (2007) Synthesis and characterization of stable ruthenabenzenes starting from HC≡CCH(OH)C≡CH. *Organometallics*, **26**(10), 2705–2713.

51 Lin, R., Zhang, H., Li, S., *et al.* (2011) New highly stable metallabenzenes via nucleophilic aromatic substitution reaction. *Chemistry: A European Journal*, **17**(15), 4223–4231.

52 Clark, G. R., Johns, P. M., Roper, W. R., *et al.* (2011) Regioselective mono-, di-, and trifunctionalization of iridabenzofurans through electrophilic substitution reactions. *Organometallics*, **30**(1), 129–138.

53 Bleeke, J. R., Xie, Y. F., Peng, W. J. and Chiang, M. (1989) Metallabenzene: Synthesis, structure, and spectroscopy of a 1-irida-3,5-dimethylbenzene complex. *Journal of the American Chemical Society*, **111**(11), 4118–4120.

54 Gilbertson, R. D., Weakley, T. J. R. and Haley, M. M. (1999) Direct synthesis of an iridabenzene from a nucleophilic 3-vinyl-1-cyclopropene. *Journal of the American Chemical Society*, **121**(11), 2597–2598.

55 Gilbertson, R. D., Lau, T. L. S., Lanza, S., *et al.* (2003) Synthesis, spectroscopy, and structure of a family of iridabenzenes generated by the reaction of Vaska-type complexes with a nucleophilic 3-vinyl-1-cyclopropene. *Organometallics*, **22**(16), 3279–3289.

56 Paneque, M., Posadas, C. M., Poveda, M. L., *et al.* (2003) Formation of unusual iridabenzene and metallanaphthalene containing electron-withdrawing substituents. *Journal of the American Chemical Society*, **125**(33), 9898–9899.

57 Álvarez, E., Paneque, M., Poveda, M. L. and Rendón, N. (2006) Formation of iridabenzenes by coupling of iridacyclopentadienes and alkenes. *Angewandte Chemie: International Edition*, **45**(3), 474–477.

58 Chin, C. S., Lee, H. and Oh, M. (1997) Reactions of iridium(III) compounds with alkynes in the presence of triethylamine: The first example of $M–CH=CH–^{+}NR_3$. *Organometallics*, **16**(4), 816–818.

59 Bleeke, J. R. (2001) Metallabenzenes. *Chemical Reviews*, **101**(5), 1205–1228.

60 Landorf, C. W. and Haley, M. M. (2006) Recent advances in metallabenzene chemistry. *Angewandte Chemie: International Edition*, **45**(24), 3914–3936.

61 Mandado, M., Otero, N. and Mosquera, R. A. (2006) Local aromaticity study of heterocycles using *n*-center delocalization indices: The role of aromaticity on the relative stability of position isomers. *Tetrahedron*, **62**(52), 12204–12210.

62 Clark, G. R., Lu, G.-L., Roper, W. R. and Wright, L. J. (2007) Stepwise reactions of acetylenes with iridium thiocarbonyl complexes to produce isolable iridacyclobutadienes and conversion of these to either cyclopentadienyliridium or tethered iridabenzene complexes. *Organometallics*, **26**(9), 2167–2177.

63 Rickard, C. E. F., Roper, W. R., Woodgate, S. D. and Wright, L. J. (2000) Electrophilic aromatic substitution reactions of a metallabenzene: Nitration and halogenation of the osmabenzene [Os{C(SMe)CHCHCHCH}I(CO)(PPh_3)$_2$]. *Angewandte Chemie: International Edition*, **39**(4), 750–752.

64 Clark, G. R., Ferguson, L. A., McIntosh, A. E., *et al.* (2010) Functionalization of metallabenzenes through nucleophilic aromatic substitution of hydrogen. *Journal of the American Chemical Society*, **132**(38), 13443–13452.

65 Menke, J. B. (1925) Brit. Pat. 235698, June 25.

66 Menke, J. B. (1925) Nitrieren mit Nitraten. *Recueil des Travaux Chimiques des Pays-Bas*, **44**(2), 141–149.

67 Menke, J. B. (1925) Nitrierung mit Nitraten: II. *Recueil des Travaux Chimiques des Pays-Bas*, **44**(3), 269–270.

68 Frogley, B. J., Dalebrook, A. F. and Wright, L. J. (2016) Regioselective nitration and/or halogenation of iridabenzofurans through electrophilic substitution. *Organometallics*, **35**(3), 400–409.

69 Einhorn, J., Demerseman, P. and Royer, R. (1983) Application en série benzofurannique d'un nouveau procédé de nitration par l'acide nitrique en présence de chlorure stannique. *Canadian Journal of Chemistry*, **61**(10), 2287–2290.

70 Dell, C. P. (2001) Science of synthesis. *Thieme Chemistry*, **10**, 11.

71 Rasala, D. and Gawinecki, R. (1992) ^{13}C NMR study of the substituent effects in ortho-substituted nitrobenzenes. *Magnetic Resonance in Chemistry*, **30**(8), 740–745.

72 Crivello, J. V. (1981) Nitrations and oxidations with inorganic nitrate salts in trifluoroacetic anhydride. *Journal of Organic Chemistry*, **46**(15), 3056–3060.

73 Gigante B., Prazeres A. O., Marcelo-Curto M. J., *et al.* (1995) Mild and selective nitration by claycop. *Journal of Organic Chemistry*, **60**(11), 3445–3447.

74 Cornélis, A., Delaude, L., Gerstmans, A. and Laszlo, P. (1988) A procedure for quantitative regioselective nitration of aromatic hydrocarbons in the laboratory. *Tetrahedron Letters*, **29**(44), 5657–5660.

75 Kurz, M. E., Zahora, E. P. and Layman, D. (1973) Benzoyl nitrate reduction with halide ions. *Journal of Organic Chemistry*, **38**(13), 2277–2281.

76 Iron, M. A., Martin, J. M. L. and van der Boom, M. E. (2003) Metallabenzene versus Cp complex formation: A DFT investigation. *Journal of the American Chemical Society*, **125**(43), 13020–13021.

77 Shi, C., Guo, T., Poon, K. C., *et al.* (2011) Theoretical study on the rearrangement of metallabenzenes to cyclopentadienyl complexes. *Dalton Transactions*, **40**(42), 11315–11320.

78 Schrock, R. R., Pedersen, S. F., Churchill, M. R. and Ziller, J. W. (1984) Formation of cyclopentadienyl complexes from tungstenacyclobutadiene complexes and the X-ray crystal structure of an η^3-cyclopropenyl complex, $W[C(CMe_3)C(Me)C(Me)](Me_2NCH_2CH_2NMe_2)Cl_3$. *Organometallics*, **3**(10), 1574–1583.

79 Jacob, V., Weakley, T. J. R. and Haley, M. M. (2002) Metallabenzenes and valence isomers: Synthesis and characterization of a platinabenzene. *Angewandte Chemie: International Edition*, **41**(18), 3470–3473.

80 Jacob, V., Landorf, C. W., Zakharov, L. N., *et al.* (2009) Platinabenzenes: Synthesis, properties, and reactivity studies of a rare class of metalla-aromatics. *Organometallics*, **28**(17), 5183–5190.

81 Jacob, V., Weakley, T. J. R. and Haley, M. M. (2002) Rearrangement of a σ-2-(Cycloprop-2-enyl)vinyl- to an η^3-Cyclopentadienylplatinum(II) Complex: Selective Protonolysis of the Platinum–Methyl Bond. *Organometallics*, **21**(24), 5394–5400.

82 Ferede, R. and Allison, N. T. (1983) Possible formation of ferrabenzene and its novel conversion to 1,3-diphenyl-2-methoxyferrocene. *Organometallics*, **2**(3), 463–465.

83 Ferede, R., Hinton, J. F., Korfmacher, W. A., *et al.* (1985) Possible formation of rhenabenzene: Lithium-halogen exchange reactions in η^1-4-bromo-1,4-diphenyl-1, 3-butadienyl ligands to form rhenabenzene and ferrabenzene. *Organometallics*, **4**(3), 614–616.

84 Wu, H.-P., Lanza, S., Weakley, T. J. R. and Haley, M. M. (2002) Metallabenzenes and valence isomers: 3: Unexpected rearrangement of two regioisomeric iridabenzenes to an (η^5-Cyclopentadienyl)iridium(I) complex. *Organometallics*, **21**(14), 2824–2826.

85 Wu, H.-P., Weakley, T. J. R. and Haley, M. M. (2005) Regioselective formation of β-alkyl-α-phenyliridabenzenes via unsymmetrical 3-vinylcyclopropenes: Probing steric and electronic influences by varying the alkyl ring substituent. *Chemistry: A European Journal*, **11**(4), 1191–1200.

86 Wu, H.-P., Ess, D. H., Lanza, S., *et al.* (2007) Rearrangement of iridabenzvalenes to iridabenzenes and/or η^5-cyclopentadienyliridium(I) complexes: Experimental and computational analysis of the influence of silyl ring substituents and phosphine ligands. *Organometallics*, **26**(16), 3957–3968.

87 Johns, P. M., Roper, W. R., Woodgate, S. D. and Wright, L. J. (2009) Carbonylchlorido(1-methylsulfanylpenta-1,3-dien-1-yl-5-ylidene)bis(triphenylphosphane)osmium(II). *Acta Crystallographica Section E*, **E65**, m1319.

88 Johns, P. M., Roper, W. R., Woodgate, S. D. and Wright, L. J. (2010) Thermal rearrangement of osmabenzenes to osmium cyclopentadienyl complexes. *Organometallics*, **29**(21), 5358–5365.

89 Bleeke, J. R. (2007) Aromatic iridacycles. *Accounts of Chemical Research*, **40**(10), 1035–1047.

90 Cao, X.-Y., Zhao, Q., Lin, Z. and Xia, H. (2013) The chemistry of aromatic osmacycles. *Accounts of Chemical Research*, **47**(2), 341–354.

91 Chen, J. and Jia, G. (2013) Recent development in the chemistry of transition metal-containing metallabenzenes and metallabenzynes. *Coordination Chemistry Reviews*, **257**(17–18), 2491–2521.

92 Paneque, M., Poveda, M. L. and Rendón, N. (2011) Synthesis and reactivity of iridacycles containing the $TpMe_2Ir$ moiety. *European Journal of Inorganic Chemistry*, **1**, 19–33.

93 Paneque, M., Posadas, C. M., Poveda, M. L., *et al.* (2007) Metallacycloheptatrienes of iridium(III): Synthesis and reactivity. *Organometallics*, **26**(14), 3403–3415.

94 Wang, T., Li, S., Zhang, H., *et al.* (2009) Annulation of metallabenzenes: From osmabenzene to osmabenzothiazole to osmabenzoxazole. *Angewandte Chemie: International Edition*, **48**(35), 6453–6456.

95 Wang, T., Zhang, H., Han, F., *et al.* (2013) Cine-substitution reactions of metallabenzenes: An experimental and computational study. *Chemistry: A European Journal*, **19**(33), 10982–10991.